Correlation among Seatbelt Load, Chest Deflection, Rib Fracture and Internal Organ Strain in Frontal Collisions with Human Body Finite Element Models

Yuichi Kitagawa, Tsuyoshi Yasuki

Abstract The chest is the most frequently injured body region in fatal and severe injury frontal collisions, and mid-sternum deflection is used as an indicator for assessing the chest injury risk. It is understood that a seatbelt load limiter helps reduce the magnitude of deflection. Therefore, the aim of this study was to examine the correlation between the seatbelt load and the mid-sternum deflection and other possible indicators for estimating chest injury risk. A total of twenty-one frontal collision simulations were conducted changing seatbelt parameters such as the load limiter value, the airbag pressure and the seatbelt type. The seatbelt load, the mid-sternum deflection, the local chest deflections, the number of rib fractures and the principal strain in the internal organs were calculated using human body finite element (FE) models: THUMS Version 4 AF05, AM50 and AM95. The results indicated that the mid-sternum deflection was not necessarily reduced by solely lowering the load limiter value but was determined by the combination of the seatbelt load and the airbag load. A significant correlation was found between the injury risk and the local deflection close to the injury location. The calculated local chest deflections at multiple locations indicated relative injury risk to the internal organs under the given loading condition.

Keywords chest deflection, frontal collision, human body FE model, seatbelt load

I. INTRODUCTION

The head and chest are the most frequently injured body regions in fatal traffic accidents. Further, vehicle occupant injuries in Japan are characterized by higher risk of chest injury compared to pedestrians and cyclists [1]. In frontal collisions, the occupant chest is protected by the seatbelt and the airbag. The seatbelt provides initial restraint to the occupant body from the beginning of collision while the airbag can distribute the restraining load over the anterior chest. The benefit of a combination of seatbelt and airbag was examined in past studies [2-3]. Since then, efforts have been made to improve these safety devices to further reduce chest injury risk. One is a seatbelt load limiter for the conventional three-point seatbelt system. Accident data analysis shows a benefit of seatbelt load limiters in frontal collisions, and a load limiter value of 4kN was proposed to achieve a good balance with the airbag [4-6]. New technologies such as a four-point seatbelt system and an inflatable seatbelt (airbelt) system also have been proposed. Past studies have shown the effectiveness of such new seatbelt systems in mitigating chest injury risk [7-8].

In regulation and assessment tests, chest deflection is commonly used as an indicator for assessing chest injury risk. In the Hybrid III dummy, deflection is measured at the mid-sternum in frontal collision tests. While the Hybrid III chest was shown to effectively simulate human chest deflection against a cylindrical impact, it is not deformable against seatbelt loading [9]. This is because the Hybrid III was originally designed assuming contact with the steering wheel hub. Because the seatbelt and the airbag are the major sources of load applied to the chest in recent vehicle models, another indicator was proposed aiming to correct the chest deflection value measured on the Hybrid III using the seatbelt load measured in the same test [10]. This indicator essentially encourages lowering the load limiter value. However, the side effect to lower the seatbelt load limiter is greater occupant forward displacement. A past study indicated a beneficial supplemental effect of an airbag with a low load limiter [11], but this study was conducted before the depowered airbag was mandated. Actual benefit of lowering the seatbelt load in a state-of-the-art restraint system is not well understood.

Yuichi Kitagawa, Ph.D. is Manager of Impact Biomechanics Group, Advanced CAE Division in TOYOTA MOTOR CORPORATION (Ph +81 565 94 2080, fax +81 565 94 2060, yuichi@kitagawa.tec.toyota.co.jp). Tsuyoshi Yasuki is Project General Manager of Advanced CAE Division in TOYOTA MOTOR CORPORATION.

The first purpose of this study was to verify the benefit of load limiters for chest protection in frontal collisions with modern restraints. Car frontal collision simulations were conducted using human body FE models to examine the correlation between the seatbelt load and mid-sternum deflection. The second purpose was to discuss possible indicators for estimating chest injury risk. The correlation between candidate indicators and injury values was examined using the simulation results. The candidate indicators were the seatbelt load and local chest deflections; the injury values were the number of rib fractures and the principal strain in the internal organs.

II. METHODS

The numerical simulations were conducted assuming a head-on collision of a mid-size sedan car against a flat rigid wall at a speed of 55km/h. The study focused on the occupant in the driver's seat wearing the seatbelt with the airbag deployed during the collision. Figure 1 shows the simulation model to be run with the LS-DYNA V971. The model represented the front part of the car cabin. Because it was assumed that deformation of the cabin was negligible, a rigid material was defined for the body side sill, pillars, front header, windshield glass, firewall and floor. Interior parts, including steering wheel and hub, instrument panel and driver seat, were considered to be deformable. Rods and brackets supporting the interior parts were also considered to be deformable. Connections among the parts such as fasteners and welds were imitated at the same locations but without breaking or tearing. These conditions are commonly used when simulating frontal impact sled tests.

This study used the THUMS Version 4 Occupant Model for representing the occupant in the driver seat. The THUMS was jointly developed by TOYOTA MOTOR CORPORATION and TOYOTA Central R&D Labs., Inc. The advanced feature new to Version 4 is internal organs. Injury risk was estimated based on the strain calculated in each organ. Bony fracture was simulated by defining a strain criterion in the material model. The impact response of the THUMS Version 4 was previously validated to human subject tests from the literature [12-13]. In addition, two new modes were validated for this study: thorax response against seatbelt loading and (simulated) airbag loading, and whole body response in frontal impact.

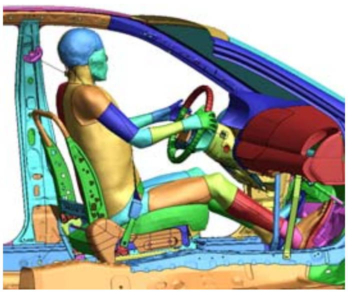

Fig. 1. Frontal Collision Simulation Model.

Validation of Thorax Response

Kent et al. [9] examined force-deflection responses of the thorax with post-mortem human subjects (PMHS). The test subjects were placed on a table top apparatus, and the anterior thorax was subjected to four loading conditions: single diagonal belt loading, double diagonal belt loading, distributed loading and a hub loading. The diagonal belt (5cm wide) represented the shoulder component of a three-point seatbelt, while a 20.3-cm-wide belt in the distributed loading imitated an airbag. In this study, force-deflection responses of the THUMS thorax were verified under the single diagonal belt loading and the distributed loading. Figure 2 shows the simulation model duplicating the loading conditions in the tests. The torso part (with the head) of THUMS Version 4 AM50 was placed on a rigid surface. The belt was modeled with shell (membrane) elements and was wrapped around the torso using a fitting tool. Seatbelt elements were used to represent the cables attached to both ends of the belt. The end of the seatbelt was pulled down through a slip-ring. Pulling force was applied to the seatbelt end simulating the force time history in the test. The chest deflection was monitored at a node on the belt over the mid-sternum; the reaction force was calculated at the rigid surface. The average stature of the fifteen subjects tested was 169.7cm with standard deviation (S.D.) of 8.5cm; the average mass value was 68.3kg with S.D. of 17.0kg. The height and the mass values of THUMS AM50 were 178cm and 74kg, respectively. These values fell within the range of S.D. of the subject size. The average age of the subjects was 69.5 with S.D. of 10.5. It was reported in the literature that the age had a small influence on the thoracic stiffness and corridors. Figure 3 compares the calculated force-deflection responses of the THUMS thorax and the test corridors. Because the THUMS calculated curve generally fell within the test corridors in both single belt loading and distributed loading, this study therefore assumed that the THUMS thorax was capable of simulating force-deflection of the human thorax against seatbelt loading and airbag loading.

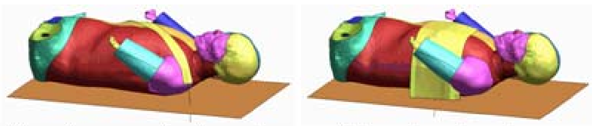

(a) Single Diagonal Belt Loading (b) Distributed Loading

Fig. 2. Validation Model for Thorax Response.

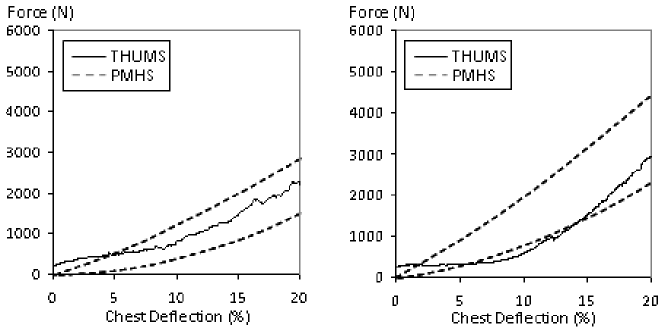

(a) Single Diagonal Belt Loading (b) Distributed Loading

Fig. 3. Comparison of Thorax Force-Deflection Responses between THUMS and PMHS.

Validation of Whole Body Response

Shaw et al. [14-16] conducted frontal impact sled tests at 40km/h with PMHS. Each subject was placed on a planar rigid seat with the head and torso supported to approximate the seated posture of a front seat occupant. The sled was equipped with a three-point seatbelt but no airbag. The shoulder and lap belts were separately adjustable, and neither a seatbelt retractor nor a load limiter was installed. A rigid knee bolster was closely placed in front of the knee. Each foot was supported by a rigid footrest with ankle straps. A total of eight subjects were tested. For three subjects, the impact kinematics was monitored using a three-dimensional motion capture system. Load cells recorded belt load, knee bolster load and other loads. The number of bony fractures was reported for all subjects. The average stature and mass of the subjects were 179cm and 76kg, respectively, while those of THUMS AM50 were 178cm and 74kg. For the THUMS validation, the bone properties were adjusted for average subject age (54.0 yrs) while the body size was not scaled. The initial posture (spine alignment) of THUMS was adjusted so as to imitate that of the test subject. Figure 4 shows the entire model used for simulating the sled tests. The seatbelt was the only device which restrained the upper body. The elongation property of the belt and the anchor locations were carefully duplicated in the model. The impact kinematics was obtained from the nodal displacement on THUMS. The seatbelt load was output from a seatbelt element close to the measuring point; the knee bolster load was calculated at the contact model defined between the knee and the bolster. Figure 5 compares the impact kinematics between the test subject and the THUMS model viewed from lateral. The figure shows trajectories of the head, T1, T8, L2, L4 and pelvis for the three subjects tested and those calculated by THUMS. The calculated trajectory fell within the range of three subjects' data from the initial point to maximum forward excursion. Figure 6 compares the time history curves of chest deflections between test subjects and the model measured at the seatbelt. Figure 7 compares the number of bony fractures between the test subjects and the model. Because the kinematics, chest deflections and number of rib fractures simulated by the model were within the range of the test data, this study therefore assumed that the THUMS thorax was capable of simulating impact kinematics of an occupant in frontal collisions and bony fractures in the thorax region.

Modeling of Restraint System

In frontal collision simulations, the THUMS Version 4 AF05, AM50 and AM95 were used for representing small female, midsize male and large male occupants. The seat position was adjusted for each occupant so as to take

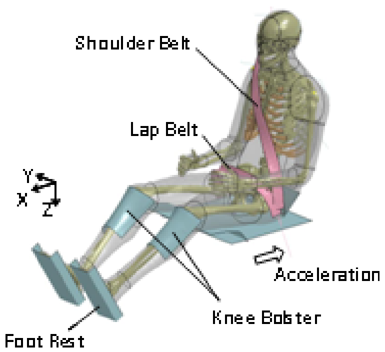

Fig. 4. Frontal Impact Sled Model.

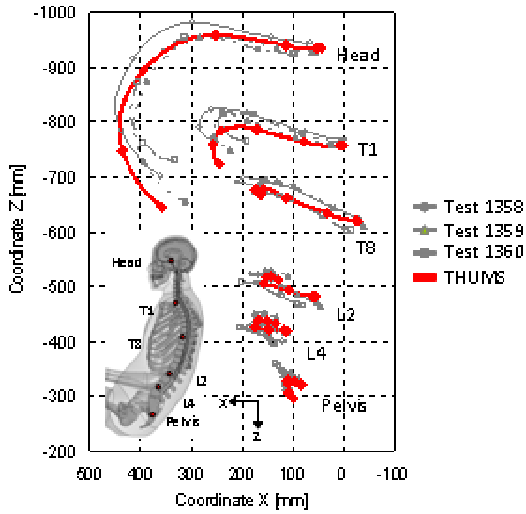

Fig. 5. Comparison of Trajectories between THUMS and PMHS.

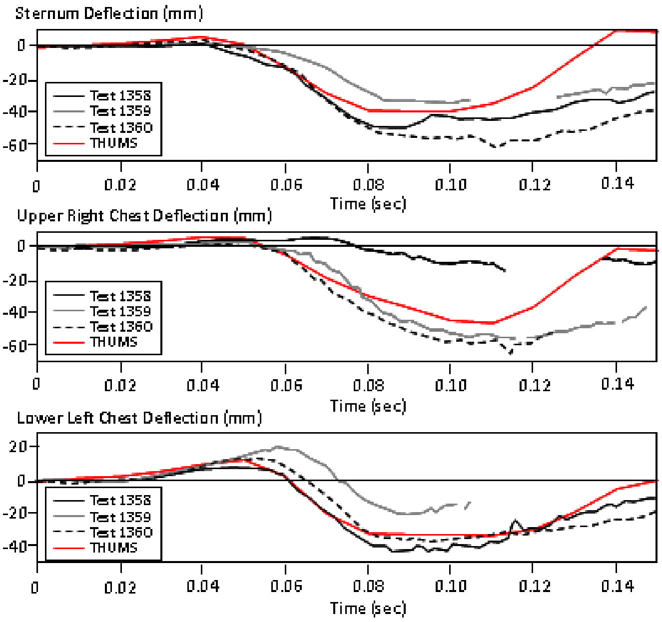

Fig. 6. Comparison of Trajectories between THUMS and PMHS.

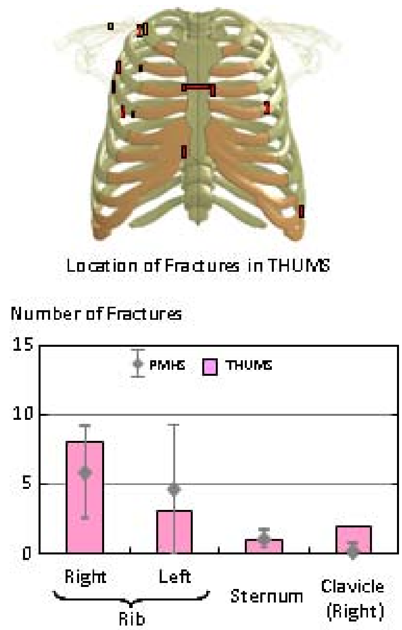

Fig. 7. Comparison of Bony Fractures in THUMS and PMHS.

a natural driving posture with both hands placed on the steering wheel and the feet on the pedals. The seat was at the mid-track position of the slide rails for AM50, 120mm forward for AF05 and 20mm rearward for AM95, respectively. A three-point seatbelt was fitted to the body surface for each occupant. One end was connected to a retractor; the other end was fixed to an anchor point on the body side sill. A slip ring was mounted to the upper part of the B-pillar; a tongue and a buckle were attached to a seat side frame. The retractor model mimicked the functions of pretensioner and load limiter. The pretensioner load was assumed to be 1.5kN in all cases, while the load limiter value was varied parametrically from 2kN to 6kN. Two other seatbelt types were also simulated in this study: a four-point seatbelt and an airbelt. The four-point seatbelt had secondary shoulder webbing crossing the original one. One end was on the floor; the other end was fixed to the body side sill through a secondary buckle. Another slip ring was mounted to the upper part of a seatback frame. The airbelt had an airbag at the shoulder part of the three-point seatbelt. Figure 8 shows the seatbelt models. Figures 9 and 10 show the driver airbag model and the airbelt model, respectively, with the initial and the deployed geometries. Initial folding of the airbags was not simulated. The study assumed that a crash sensor activated the restraint system at 0.018 seconds after the initiation of frontal collision. Deployment of the driver airbag was simulated using a control volume method in LS-DYNA.

(a) Three-Point Seatbelt (b) Four-Point Seatbelt (c) Airbelt

Fig. 8. Seatbelt Models.

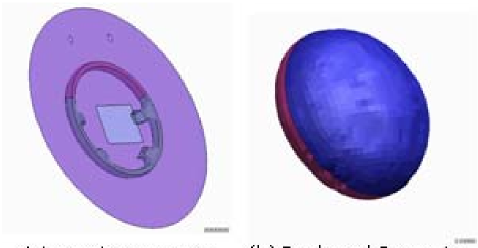

(a) Initial Geometry (b) Deployed Geometry

Fig. 9. Driver Airbag Model.

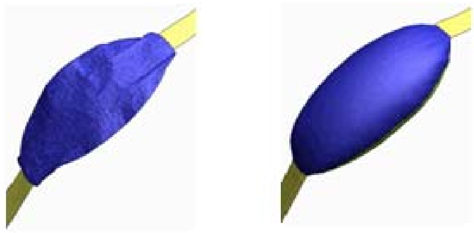

(a) Initial Geometry (b) Deployed Geometry

Fig. 10. Airbelt Model.

Simulation Matrix

The study consisted of three parts. For the first part, all three models (AF05, AM50 and AM95) were restrained with the three-point belt with the load limiter value varied from 2kN to 6kN. The second and third parts focused on the AM50 occupant. In the second part, the airbag pressure was varied with load limiter value to change load sharing between two systems: increased airbag load with decreased seatbelt load or decreased airbag load with increased seatbelt load. In the third part, the four-point seatbelt and the airbelt were installed. A load limiter value of 2kN was assumed for each retractor of the four-point seatbelt. The total restraining load was equivalent to that of the three-point seatbelt. A load limiter value of 4kN was assumed for the retractor of the airbelt. Table I summarizes the simulation matrix. A total of twenty-one simulations were conducted. Figure 11 shows nine points on the thorax at which local deflections were calculated. Note combinations of anterior points and posterior points. The deflection was calculated as a percentage of distance change between the anterior point and the posterior point. Figure 12 shows the internal organs of the three models. In frontal collisions, injuries are commonly found in the lungs, heart, spleen and liver. The maximum principal strains of these organs were calculated to estimate injury risk to these organs. The seatbelt load was output from an element on the webbing between the slip ring and the shoulder. The airbag load was calculated as a contact force between the airbag and the anterior thorax. The forward displacement of thorax was monitored at T7.

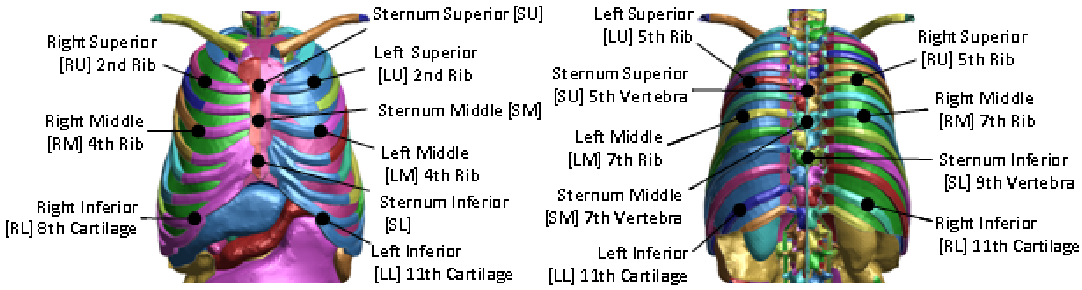

(a) Anterior View (b) Posterior View

Fig. 11. Calculation Points of Local Chest Deflections.

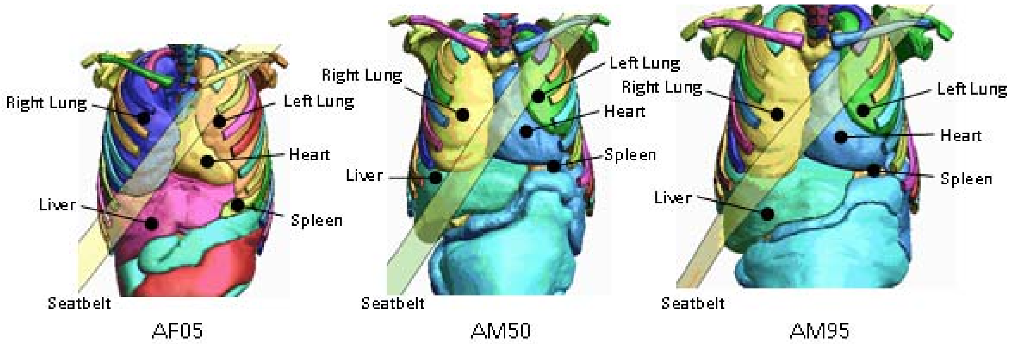

Fig. 12. Internal Organs in THUMS.

TABLE I
Simulation Matrix

<table>
<tr><th>Case</th><th>Occupant</th><th>Seatbelt</th><th>Pretensioner</th><th>Load Limiter</th><th>Airbag</th><th>Velocity</th></tr>
<tr><td>1</td><td rowspan="5">AF05</td><td rowspan="19">Three-Point</td><td rowspan="21">1.5kN (Outer)</td><td>2kN</td><td rowspan="15">Standard Pressure</td><td rowspan="21">55km/h</td></tr>
<tr><td>2</td><td>3kN</td></tr>
<tr><td>3</td><td>4kN</td></tr>
<tr><td>4</td><td>5kN</td></tr>
<tr><td>5</td><td>6kN</td></tr>
<tr><td>6</td><td rowspan="5">AM50</td><td>2kN</td></tr>
<tr><td>7</td><td>3kN</td></tr>
<tr><td>8</td><td>4kN</td></tr>
<tr><td>9</td><td>5kN</td></tr>
<tr><td>10</td><td>6kN</td></tr>
<tr><td>11</td><td rowspan="5">AM95</td><td>2kN</td></tr>
<tr><td>12</td><td>3kN</td></tr>
<tr><td>13</td><td>4kN</td></tr>
<tr><td>14</td><td>5kN</td></tr>
<tr><td>15</td><td>6kN</td></tr>
<tr><td>16</td><td rowspan="6">AM50</td><td>2kN</td><td>Pressure x1.4</td></tr>
<tr><td>17</td><td>3kN</td><td>Pressure x1.2</td></tr>
<tr><td>18</td><td>5kN</td><td>Pressure x0.8</td></tr>
<tr><td>19</td><td>6kN</td><td>Pressure x0.6</td></tr>
<tr><td>20</td><td>Four-Point</td><td>2kN+2kN</td><td rowspan="2">Standard Pressure</td></tr>
<tr><td>21</td><td>Airbelt</td><td>4kN</td></tr>
</table>

III. RESULTS

Impact kinematics of different size occupants with different load limiter values, airbag pressures and seatbelt types are shown in the Appendix. Figure 13 shows the impact kinematics of the AM50 occupant at 0.09 sec with load limiter values of 2, 4 and 6kN (Cases 6, 8 and 10). Greater forward excursion was found with a load limiter of 2kN compared to those in the other cases. Airbag deformation appeared greatest with a load limiter of 2kN. Figure 14 shows the thorax region in the mid-sagittal section view. The chest contacted the lower part of the steering wheel with a load limiter of 2kN, while no steering wheel contact occurred in the other cases. Figure 15 shows the skeletal deformation of the thorax in Cases 6, 8 and 10. No rib fracture was predicted in Case 6; a fracture to left rib 1 was predicted in Case 8; fractures to left ribs 1-4 were predicted in Case 10. Figure 16 shows distribution of the maximum principal strain of the internal organs in Case 8. High strain values were found at the anterior border of the right lung, medial surface of the left lung, superior region of the heart (around the insertion area of the aorta), medial surface of the spleen and the superior region of the liver

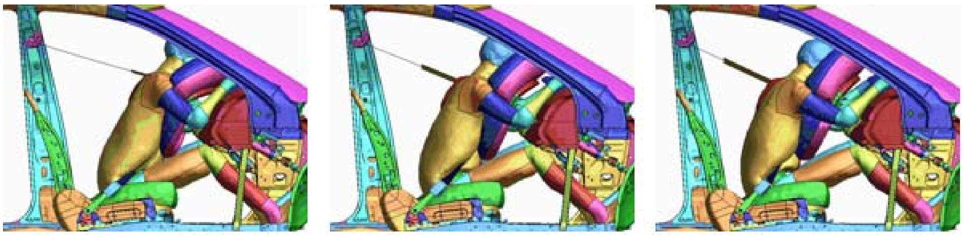

Case 6 (Load Limiter: 2 kN) Case 8 (Load Limiter: 4 kN) Case 10 (Load Limiter: 6 kN)

Fig. 13. Impact Kinematics of THUMS V4 AM50 Occupant (0.09 sec).

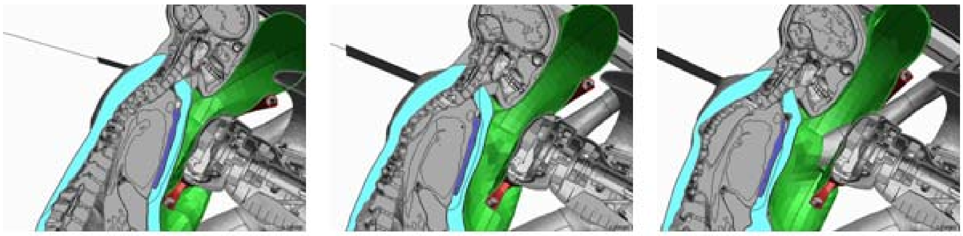

Case 6 (Load Limiter: 2 kN) Case 8 (Load Limiter: 4 kN) Case 10 (Load Limiter: 6 kN)

Fig. 14. Mid-Sagittal Section View of Thorax Region –AM50- (0.09 sec).

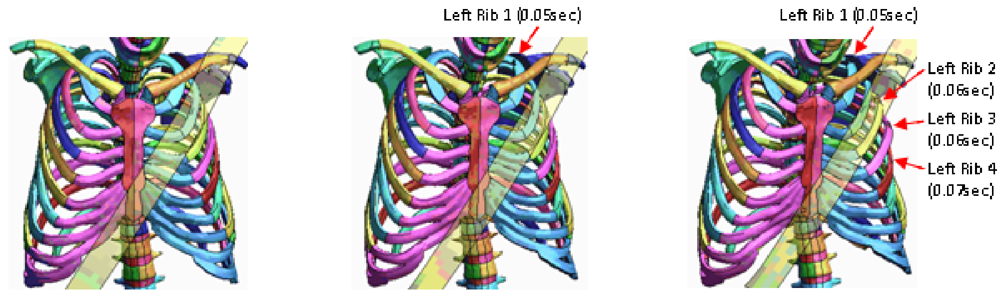

Case 6 (Load Limiter: 2 kN) Case 8 (Load Limiter: 4 kN) Case 10 (Load Limiter: 6 kN)

Fig. 15. Skeletal Deformation of Thorax (0.09 sec) and Predicted Rib Fractures.

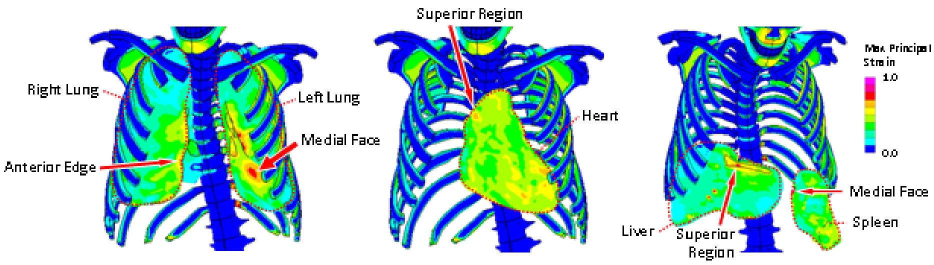

Right and Left Lungs Heart Spleen and Liver

Fig. 16. Distribution of Maximum Principal Strain of Internal Organs (Case 8, 0.09 sec).

(near the coronary ligament). Figure 17 compares the kinematics among AF05, AM50 and AM95 with a load limiter of 4kN at the time of maximum forward excursion of the chest (Cases 3, 8 and 13). Flexion of the AF05 upper body was smaller relative to the AM50 and AM95. The sagittal section of the thorax region is shown in Figure 18. The chest contacted the lower part of the steering wheel in AM95 even with a load limiter of 4kN. Figure 19 shows the mid-sagittal section view of the AM50 thorax at 0.09 sec with varied load sharing between seatbelt and airbag for study Part 2 (Cases 16, 8 and 19). Some distance was left between the chest and the steering wheel in all three cases. Figure 20 shows the skeletal deformation of the thorax for these cases. One rib fracture was predicted in Cases 16 and 8 while three fractures were predicted in Case 19. Figure 21 compares the impact kinematics between the three-point seatbelt, four-point seatbelt and airbelt for study Part 3 (Cases 8, 20 and 21). No significant difference was found in upper body excursion.

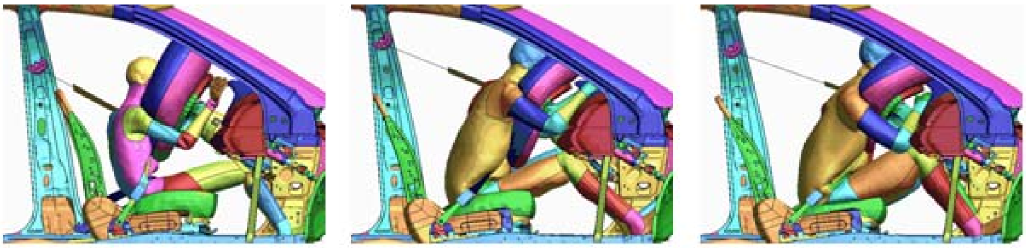

Case 3 (AF05, Load Limiter: 4 kN) Case 8 (AM50, Load Limiter: 4 kN) Case 13 (AM95, Load Limiter: 4 kN)

Fig. 17. Comparison of Impact Kinematics among AF05, AM50 and AM95.

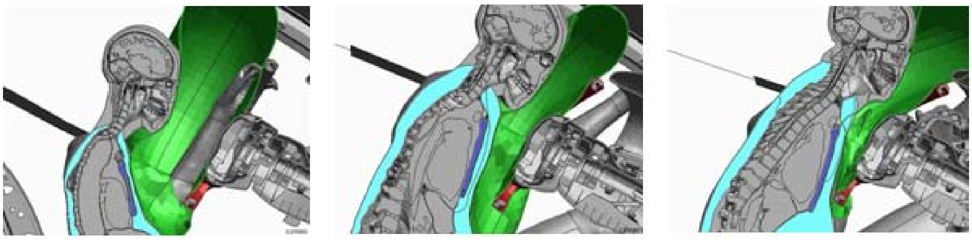

Case 3 (AF05, Load Limiter: 4 kN) Case 8 (AM50, Load Limiter: 4 kN) Case 13 (AM95, Load Limiter: 4 kN)

Fig. 18. Comparison of Thorax Mid-Sagittal Section View among AF05, AM50 and AM95.

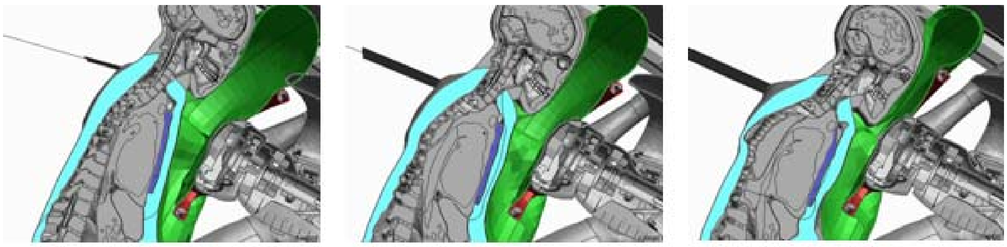

Case 16 (Load Limiter: 2 kN, Airbag Pressure x1.4) Case 8 (Load Limiter: 4 kN Airbag Pressure Standard) Case 19 (Load Limiter: 6 kN, Airbag Pressure x0.6)

Fig. 19. Sagittal Section View of Thorax Region –AM50 with Airbag Pressure Changed- (0.09 sec).

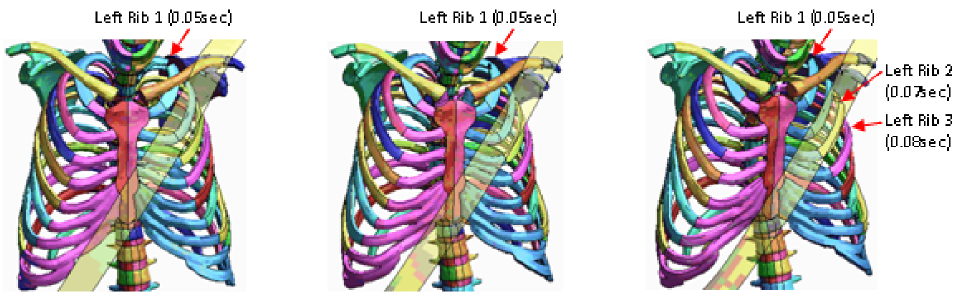

Case 16 (Load Limiter: 2 kN, Airbag Pressure x1.4) Case 8 (Load Limiter: 4 kN Airbag Pressure Standard) Case 19 (Load Limiter: 6 kN, Airbag Pressure x0.6)

Fig. 20. Skeletal Deformation of Thorax (0.09 sec) and Predicted Rib Fractures.

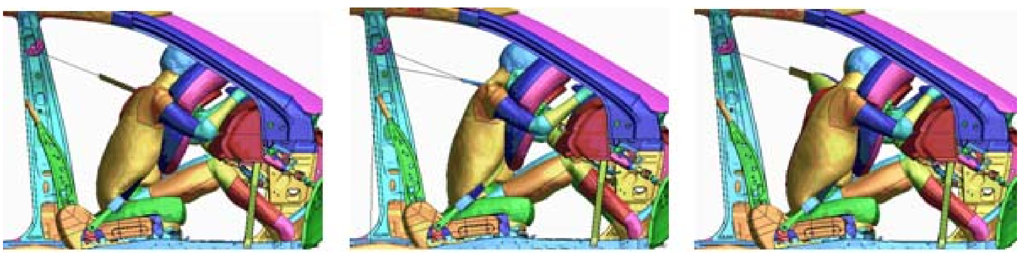

Case 8 (Three-Point Seatbelt) Case 20 (Four-Point Seatbelt) Case 21 (Airbelt)

Fig. 21. Impact Kinematics of THUMS V4 AM50 Occupant with Different Seatbelt Type (0.09 sec).

Time history curves for seatbelt load, airbag load, chest deflection and forward displacement of the chest are plotted in the Appendix. Figure 22 plots the time history curves of seatbelt and airbag loads for the AM50 occupant with a load limiter value of 4kN (Case 8). The seatbelt load rose at 0.018 sec when the pretensioner was activated. Its magnitude increased as the occupant body moved forward. After reaching 4kN, the seatbelt load held constant as evidenced by the flat-topped profile. The airbag load rose at around 0.04 sec and increased as the upper body engaged it, showing a triangular profile with a maximum peak at around 0.08 sec. Figure 23 plots the time history curve of chest deflection at the mid sternum (SM) for the same case (Case 8). An initial rise was due to the seatbelt load but later was increased by both seatbelt and airbag loads. The deflection profile had a peak at around 0.08 sec corresponding to that of airbag load. Figure 24 plots the maximum values of local chest deflections for the same case (Case 8). Greater deflection was noted along the shoulder belt path from left superior (LU) to right inferior (RL). Figure 25 plots the time history curves of the maximum principal strain in the lungs, heart, spleen and liver. The strain values were calculated at locations specified in Figure 16. The maximum values of seatbelt load, airbag load, chest deflections, forward chest displacement, internal organ strain and the number of rib fractures are summarized in the Appendix.

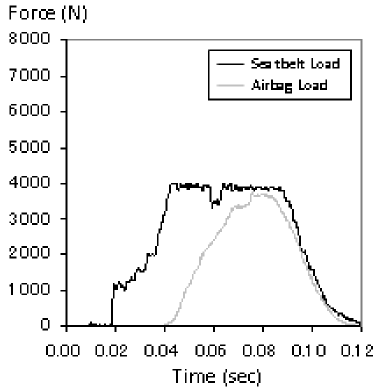

Fig. 22. Seatbelt Load and Airbag Load (Case 8).

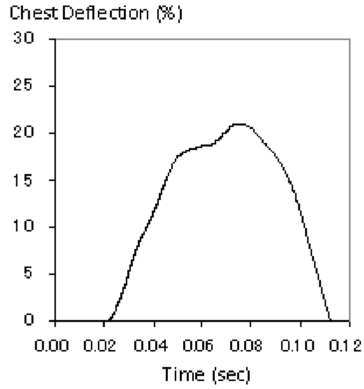

Fig. 23. Chest Deflection (Case 8).

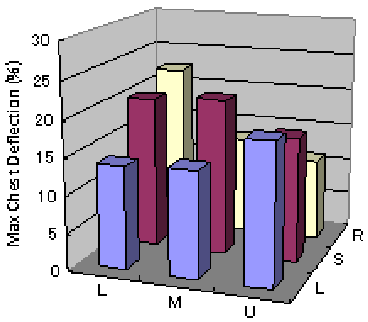

Fig. 24. Local Chest Deflection (Case 8).

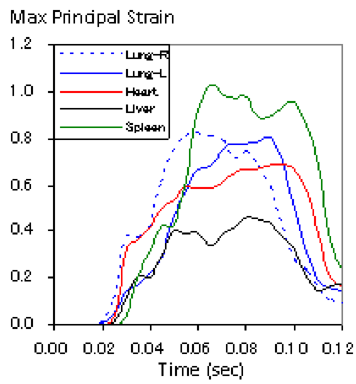

Fig. 25. Strain of Internal Organs (Case 8).

Figure 26 plots the maximum values of chest deflection (SM) and forward chest displacement with respect to the load limiter values for AF05, AM50 and AM95 (Cases 1-15). As the load limiter value was lower in AF05, the chest deflection was smaller but the forward displacement was greater. For AM50 and AM95, a similar trend was found in forward displacement. However, the chest deflection was not necessarily the smallest at the lowest load limiter value. In AM50, the chest deflection with a 2kN load limiter was almost the same as with 3kN. In AM95, the chest deflection with a 2kN load limiter was greater than with 3kN or 4kN. It should be noted that the chest reached the lower part of the steering wheel in these cases. Figure 27 plots the maximum values of seatbelt load, airbag load, chest deflection (SM) and forward chest displacement for the AM50 cases with the airbag pressure changed (Cases 8, 16-19). With smaller load limiter value the seatbelt load decreased while the airbag load increased. Relatively small difference was found in chest deflection and forward displacement of the chest among the cases.

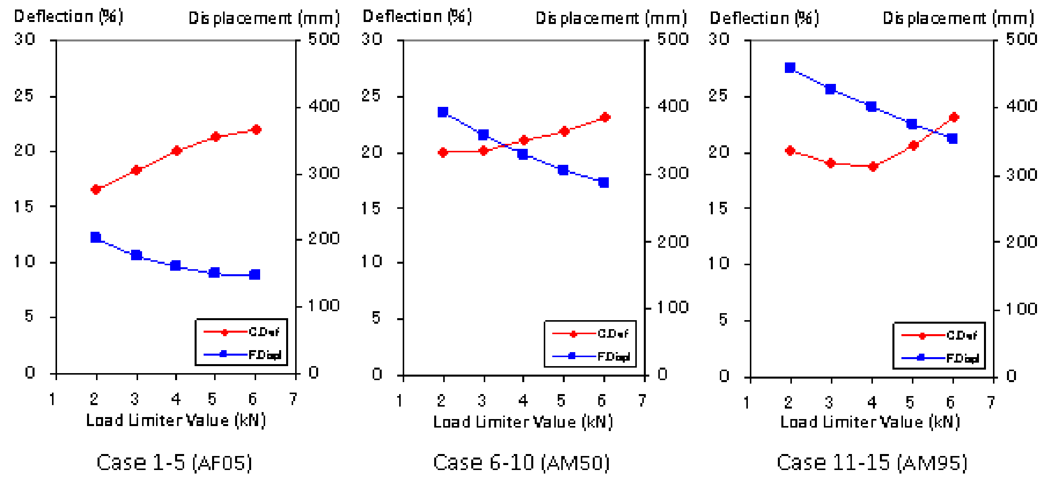

Fig. 26. Chest Deflection and Forward Displacement w.r.t. Load Limiter Value.

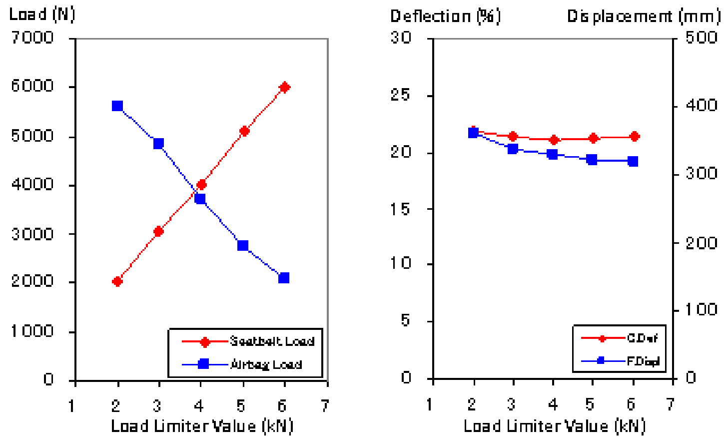

Fig. 27. Seatbelt Load, Airbag Load, Chest Deflection and Forward Displacement w.r.t. Load Limiter Value with variable airbag pressure.

Figure 28 compares the maximum values of seatbelt load, airbag load and chest deflection among the AM50 cases with three-point seatbelt, four-point seatbelt and airbelt (Cases 8, 20 and 21). The seatbelt loads were similar among these three cases in part because the same load limiter values were given. The airbag load decreased with the four-point belt (Case 20) and decreased further with the airbag (Case 21). Similarly, smaller chest deflection was found with the four-point belt and airbelt compared to the standard restraints.

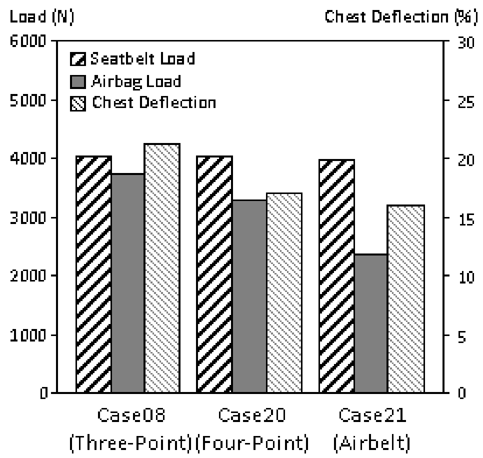

Fig. 28. Comparison of Seatbelt Load, Airbag Load, Chest Deflection among Seatbelt Types.
(Note that the seatbelt load in Case 20 was the sum of two shoulder belts.)

The correlation between candidate indicators and injury values was examined. The candidate indicators were the seatbelt load and local chest deflections; the injury values were the number of rib fractures and internal organ principal strain. Table II summarizes the correlation for the AM50 cases (Cases 6-10 and 16-21). The correlation coefficients and p-values were calculated using the Pearson product-moment correlation. The study assumed that there was a significant correlation between the indicator and the injury value when the coefficient value was greater than or equal to 0.7 with a p-value smaller than 0.05. A negative coefficient value indicated that the injury value decreased when the indicator increased. This was a second order effect possibly due to the incompressible characteristics of the internal organs such that a compressive load to one side caused expansion on the other side. In this study, therefore, only positive coefficient values were discussed.

With the number of rib fractures, a significant correlation was found for the seatbelt load, left superior deflection (LU) and left middle deflection (LM). The left superior deflection (LU) has the highest correlation among three indicators. With the strain of the right lung, a significant correlation was found for the right inferior deflection (RL), mid sternum deflection (SM) and inferior sternum deflection (SL). With the strain of the left lung, a significant correlation was found for the right inferior deflection (RL), mid sternum deflection (SM) and left superior deflection (LU). The heart strain correlated with the right inferior deflection (RL), mid sternum deflection (SM) and inferior sternum deflection (SL). With the spleen strain, the seatbelt load and left superior deflection (LU) showed a significant correlation. Deflections at the right inferior (RL), mid sternum (SM) and inferior sternum (SL) showed a significant correlation with the liver strain.

TABLE II
Correlation between Indicators and Injury Values

Injury Value	Correlation	Indicators									
		Seatbelt Load	RU	RM	RL	SU	SM	SL	LU	LM	LL
Rib FX	Coefficient	0.84	-0.86	-0.68	0.58	0.00	0.60	0.53	0.95	0.84	-0.58
	p-value	0.0000	0.0000	0.0007	0.0056	0.9840	0.0041	0.0143	0.0000	0.0000	0.0062
Lung-R	Coefficient	0.16	-0.30	-0.03	0.95	-0.47	0.91	0.81	0.36	0.33	-0.31
	p-value	0.6366	0.3636	0.9310	0.0000	0.1842	0.0001	0.0025	0.2829	0.3170	0.3487
Lung-L	Coefficient	0.52	-0.69	-0.49	0.83	-0.26	0.79	0.64	0.76	0.64	-0.65
	p-value	0.0988	0.0183	0.1241	0.0015	0.4393	0.0040	0.0330	0.0065	0.0356	0.0309
Heart	Coefficient	0.11	-0.24	0.04	0.96	-0.55	0.93	0.86	0.32	0.32	-0.27
	p-value	0.7533	0.4764	0.9184	0.0000	0.0.0806	0.0000	0.0007	0.3295	0.3307	0.4276
Spleen	Coefficient	0.80	-0.93	-0.88	0.28	0.07	0.24	0.11	0.84	0.53	-0.79
	p-value	0.0031	0.0000	0.0004	0.4040	0.8297	0.4849	0.7367	0.0012	0.0921	0.0037
Liver	Coefficient	0.05	-0.07	0.15	0.77	-0.33	0.77	0.76	0.31	0.55	-0.05
	p-value	0.8768	0.8289	0.6648	0.0060	0.3162	0.0051	0.0065	0.3599	0.0816	0.8783

IV. DISCUSSION

The first finding in this study was that a lower load limiter value did not necessarily give the smallest chest deflection. A lower seatbelt load itself reduced the chest deflection but also increased the forward displacement of the chest (Cases 1-15). In AM50 and AM95, a greater forward displacement caused contact between the chest and the steering wheel later in the restraint phase (Cases 6, 11 and 12). When the airbag pressure was changed to help reduce forward chest displacement (Cases 16-19), the resultant chest deflection was not smaller with a reduced load limiter. These results derived from the fact that both seatbelt load and airbag load contributed to chest deflection. Assuming an equivalent forward motion of the chest, the load limiter value mostly changes the ratio of load sharing between the seatbelt and the airbag. A higher seatbelt load increased the left superior deflection (LU), and a greater deflection raises fracture risk. This was evidenced by Cases 18 and 19, in which multiple rib fractures were predicted at load limiter values of 5 and 6kN. Because little difference was found among 2, 3 and 4kN (Cases 16, 17 and 8), a load limiter value of 4kN appeared low enough in terms of local chest deflection and rib fracture risk.

The chest deflections with the four-point seatbelt and the airbelt were smaller than that with the three-point seatbelt despite similar load limiter values (Cases 20 and 21). The benefit of the four-point seatbelt was to engage both shoulders. It was effective for restraining the occupant due to the relatively high stiffness of the shoulder-clavicle area compared to the chest. The beneficial feature of the airbelt was its increased contact area with the shoulder-chest. Additionally, the airbelt deployment worked as a secondary pretensioner and separated the lower portion of the shoulder belt from the inferior chest. The performance of the four-point seatbelt and airbelt could change depending on factors such as the rigidity of the slip ring for the secondary belt and the inflator power. The study results showed a potential effectiveness of the four-point seatbelt and airbelt in reducing chest deflection under the simulated conditions.

The seatbelt load showed a significant correlation with the number of rib fractures and the principal strain of spleen but not with strain of the other internal organs. The correlations with the local chest deflections varied among the internal organs. Specifically, the strain of an internal organ correlated with the local deflection around that part. Regarding rib fractures, the seatbelt load could be used to estimate a fracture risk at the left superior area only. The occupant model used in this study assumed an adult person at middle age. Elderly occupants are likely to sustain rib fractures along the seatbelt not only at the superior area but also at the inferior area [17]. The injury risk to the inferior chest could be missed by monitoring only the seatbelt load. The skeletal parts and internal organs are located at various areas of the chest. The study results suggested that the chest injury risk should be assessed by monitoring deflections at multiple points on the chest.

The study has the following limitations. The model validations were conducted for the limited number of literature data. The calculated impact kinematics, force-deflection responses and number of bony fractures were compared to the test data, but the validity of calculated internal organ strain was not examined. The study assumed that the calculated strain indicated relative loading severity among internal organs. The model simulated a head-on collision of a vehicle with a single deceleration pulse without deformation of the cabin structure. It did not necessarily represent a general trend of injury scenarios in actual car crashes. The study results indicated a possible trend of occupant chest injury under the simulated impact conditions.

V. CONCLUSIONS

The study conducted frontal collision simulations using the THUMS Version 4 AF05, AM50 and AM95 Occupant Models in order to examine the effectiveness of seatbelt load limiters in reducing chest deflection and to analyze the correlation between chest injury indicators and injury values. The simulation results indicated that lowering the load limiter value, for instance from 4 kN to 2 kN, did not necessarily reduce the chest deflection. The chest deflection was not dominated by the seatbelt load but generated by both seatbelt load and airbag load. Even with the same load limiter value, smaller chest deflection was generated with the four-point seatbelt and the airbelt. The seatbelt load showed a significant correlation with the number of rib fractures at the left superior area and with the principal strain of the spleen, but not with strains in the other internal organs. The internal organ strain generally correlated with the deflection at the area of the site. Neither the chest deflection at a particular location nor the seatbelt load calculated at the shoulder indicated what internal organ was likely to sustain injury. The calculated local chest deflections at multiple locations showed relative injury risk to the internal organs under the given loading condition.

VI. REFERENCES

[1] National Policy Agency (Japan), Annual Report of Traffic Accidents Situation in 2011 (in Japanese) Internet: http://www.npa.go.jp/koutsuu/index.htm, February 23, 2012.

[2] Kallieris D, Rizzetti A, Mattern R, Morgan R, Eppinger R, Keenan L, On the Synergism of the Driver Air Bag and the 3-Point Belt in Frontal Collisions, *Society of Automotive Engineers, inc.*, 952700, 389-401, 1995.

[3] Augenstein J, Perdeck E, Bowen J, Stratton J, Horton T, Singer M, Rao A, Digges K, Malliaris A, Injury Patterns Among Belted Drivers Protected by Air Bags in 30 to 35 mph Crashes, *Society of Automotive Engineers, inc.*, 1999-01-1062, 1999.

[4] Lu H, Andreen M, Fausst D, Furton L, Holcombe S, Kohoyda-Inglis C, Putala B, Yee J, Wang S, Safety Belt and Occupant Factors Influencing Thoracic & Upper Abdominal Injuries in Frontal Crashes, *Society of Automotive Engineers, inc.*, 2011-01-1129, 2011.

[5] Foret-Bruno J-Y, Trosseille X, Le Coz J-Y, Bendjellal F, Steyer C, Phalempin T, Villeforceix D, Dandres P, Got C. Thoracic Injury Risk in Frontal Car Crashes with Occupant Restrained with Belt Load Limiter. *Society of Automotive Engineers, inc.*, 983166, 389-401, 1998.

[6] Foret-Bruno J-Y, Trosseille X, Page Y, Huere J-F, Le Coz J-Y, Bendjellal F, Diboine A, Phalempin T, Villeforceix D, Baudrit P, Guillemot H, Coltat J-C, Comparison of Thoracic Injury Risk in Frontal Car Crashes for Occupant Restrained without Belt Load Limiters and Those Restrained with 6kN and 4kN Belt Load Limiters, *Stapp Car Crash Journal*, 45: 205-224, 2001.

[7] Natalini T, Carr K, Vala M, Boroughf W, Variables Influencing Shoulder Belt Positioning of Four Point Safety Belts, *Society of Automotive Engineers, inc.*, 2001-01-0382, 2001.

[8] Sundararajan S, Rouhana S, Board D, DeSmet E, Prasad P, Rupp J, Miller C, Schneider L, Biomechanical Assessment of a Rear-Seat Inflatable Seatbelt in Frontal Impacts, *Stapp Car Crash Journal*, 55: 161-197, 2011.

[9] Kent R, Lessley D, Sherwood C, Thoracic Response to Dynamic, Non-Impact Loading from a Hub, Distributed Belt, Diagonal Belt, and Double Diagonal Belts, *Stapp Car Crash Journal*, 48: 495-519, 2004.

[10] Petitjean A, Baudrit P, Trosseille X, Thoracic Injury Criterion for Frontal Crash Applicable to All Restraint Systems, *Stapp Car Crash Journal*, 47: 323-348, 2003.

[11] Mertz H, Williamson J, Lugt D, The Effect of Limiting Shoulder Belt Load with Air Bag Restraint, *Society of Automotive Engineers, inc.*, 950886, 1995.

[12] Shigeta K, Kitagawa Y, Yasuki T, Development of Next Generation Human FE Model Capable of Organ Injury Prediction, *Proceedings of the 21st ESV Conference*, 09-0111, 2009.

[13] Watanabe R, Katsuhara T, Miyazaki H, Kitagawa Y, Yasuki T, Research of the Relationship of Pedestrian Injury to Collision Speed, Car-type, Impact Location and Pedestrian Sizes using Human FE Model (THUMS Version 4), *Stapp Car Crash Journal*, 56: 269-321, 2012.

[14] Shaw G, Parent D, Purtsezov S, Lessley D, Kerrigan J, Shin J, Crandall J, Zama Y, Ejima S, Kamiji K, Yasuki T, Frontal Impact PMHS Sled Tests for FE TORSO Model Development, *Proceedings of IRCOBI Conference, York, United Kingdom*, 2009.

[15] Shaw G, Parent D, Purtsezov S, Lessley D, Crandall J, Kent R, Guillemot H, Ridella S, Takhounts E, Martin P, Impact Response of Restrained PMHS in Frontal Sled Tests: Skeletal Deformation Patterns Under Seat Belt Loading, *Stapp Car Crash Journal*, 53: 1-48, 2009.

[16] Ash J, Lessley D, Forman J, Zhang Q, Shaw G, Crandall J, Whole-Body Kinematics: Response Corridors for Restrained PMHS in Frontal Impacts, *Proceedings of IRCOBI Conference*, Dublin, Ireland, 141-154, 2012.

[17] Shimamura M, Ohhashi H, Yamazaki M, The effects of occupant age on patterns of rib fractures to belt-restrained drivers and front passengers in frontal crashes in Japan, *Stapp Car Crash Journal*, 47: 349-365, 2003.

VII. Appendix

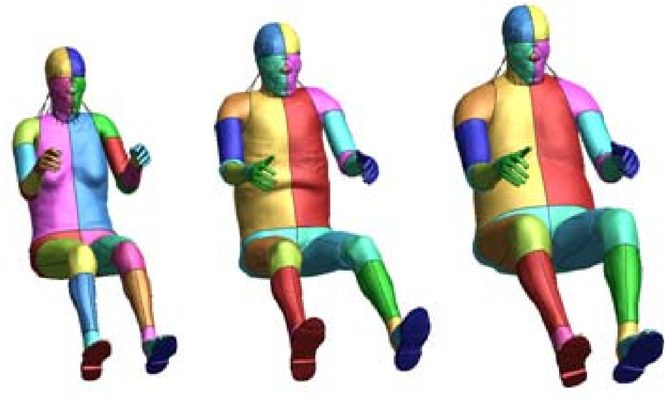

Fig. A1. THUMS Version 4 Occupant Models

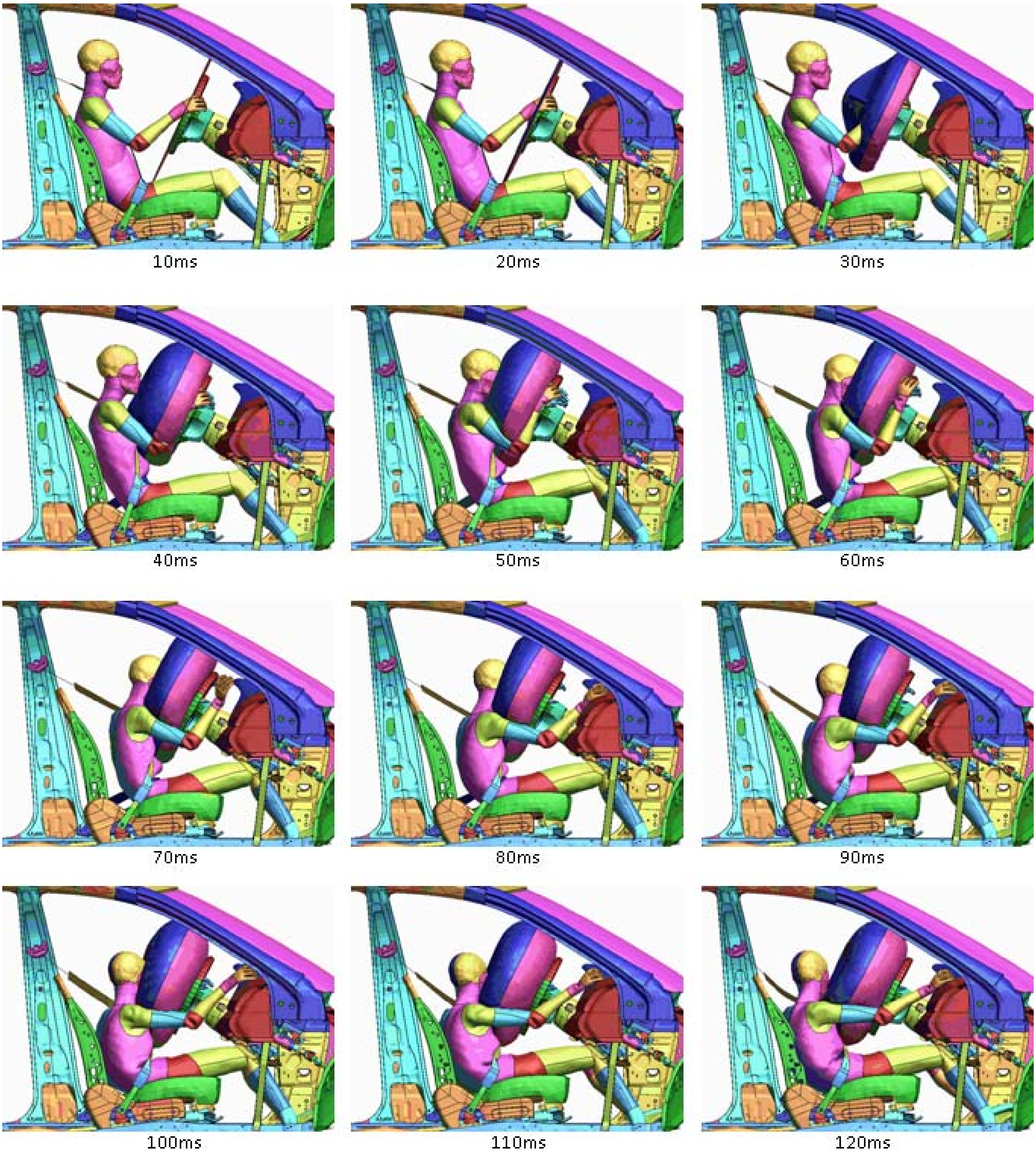

Fig. A2. Occupant Kinematics of AF05 Occupant with 4 kN Load Limiter (Case 3).

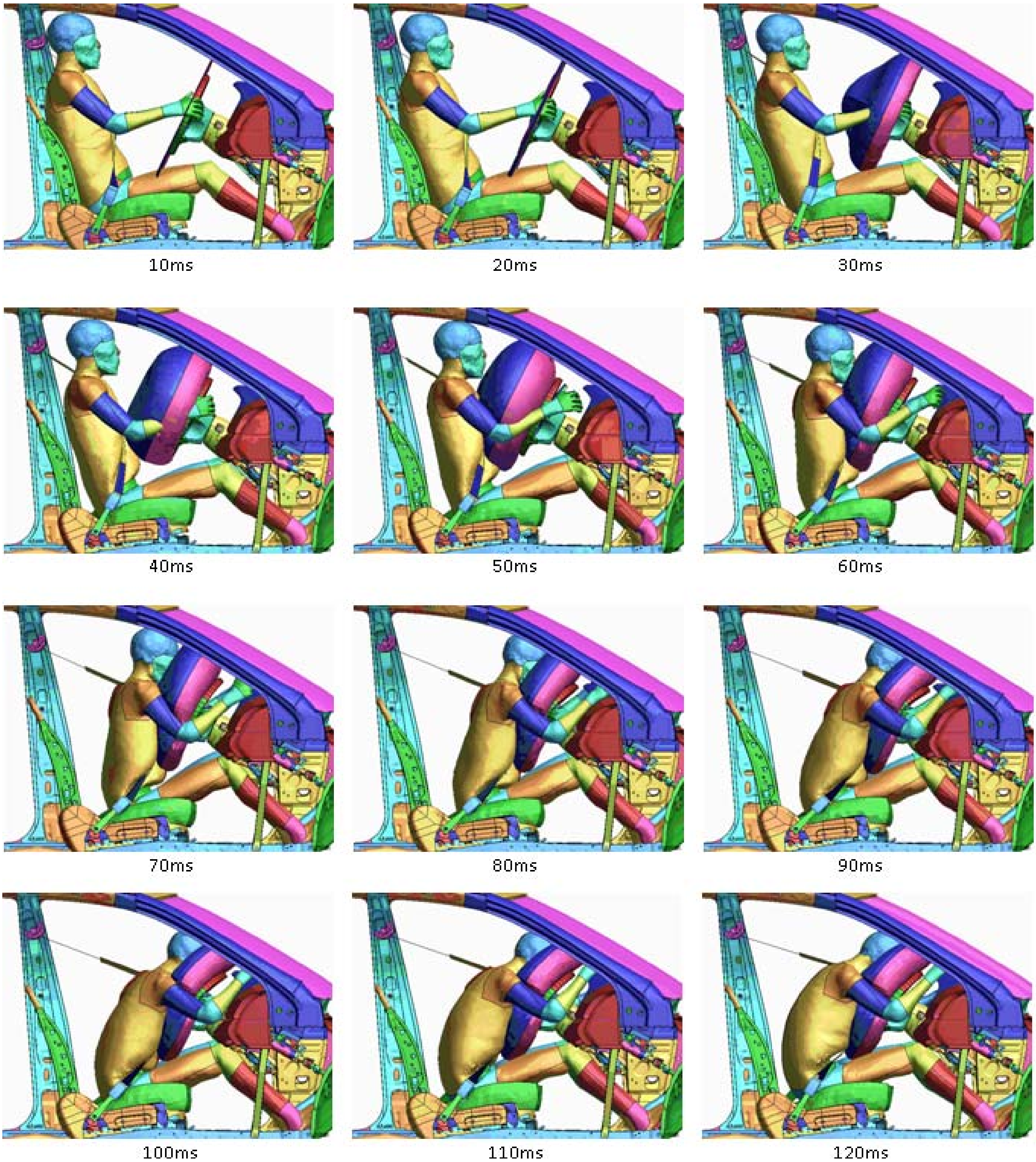

Fig. A3. Occupant Kinematics of AM50 Occupant with 4 kN Load Limiter (Case 8).

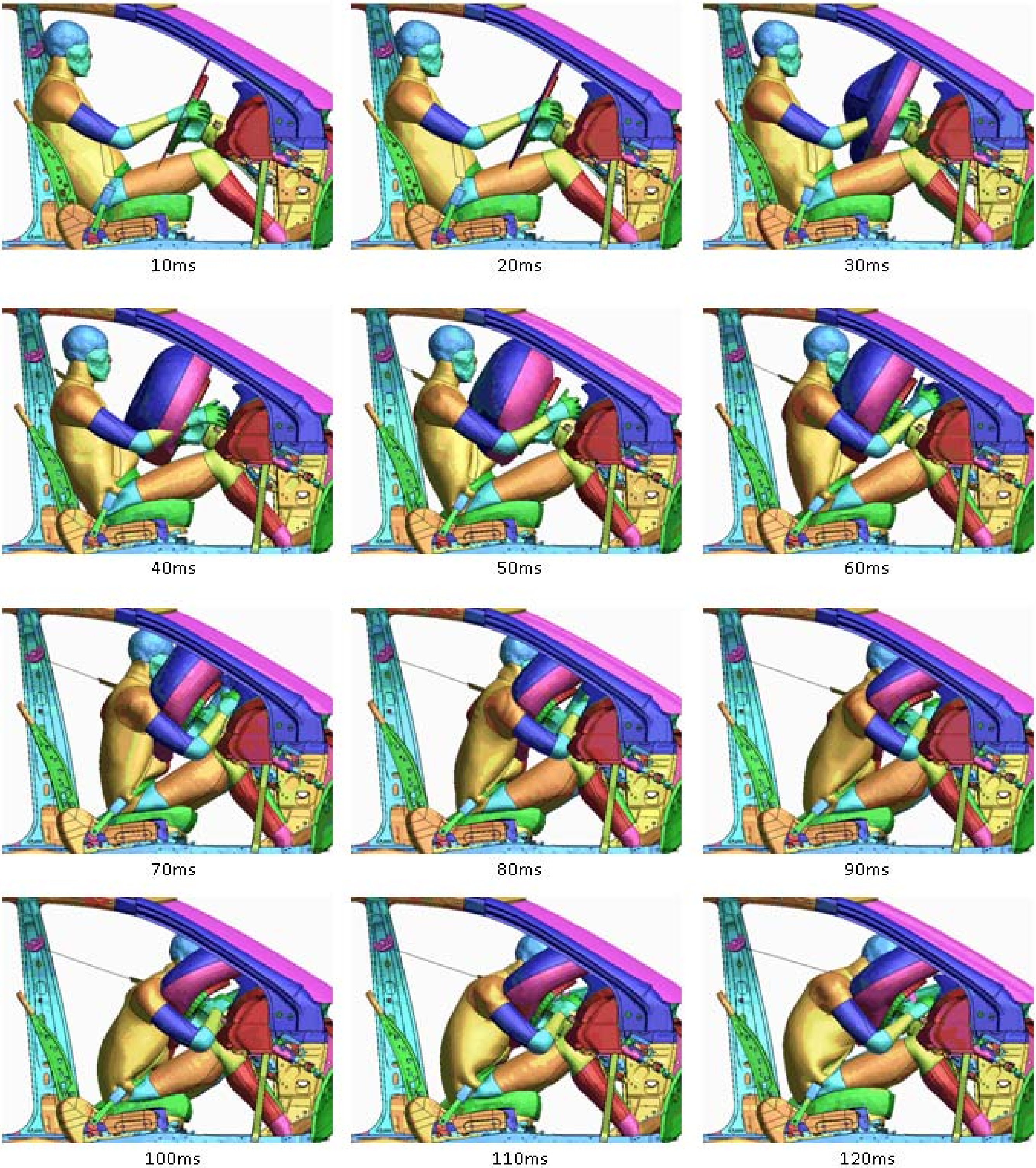

Fig. A4. Occupant Kinematics of AM95 Occupant with 4 kN Load Limiter (Case 13).

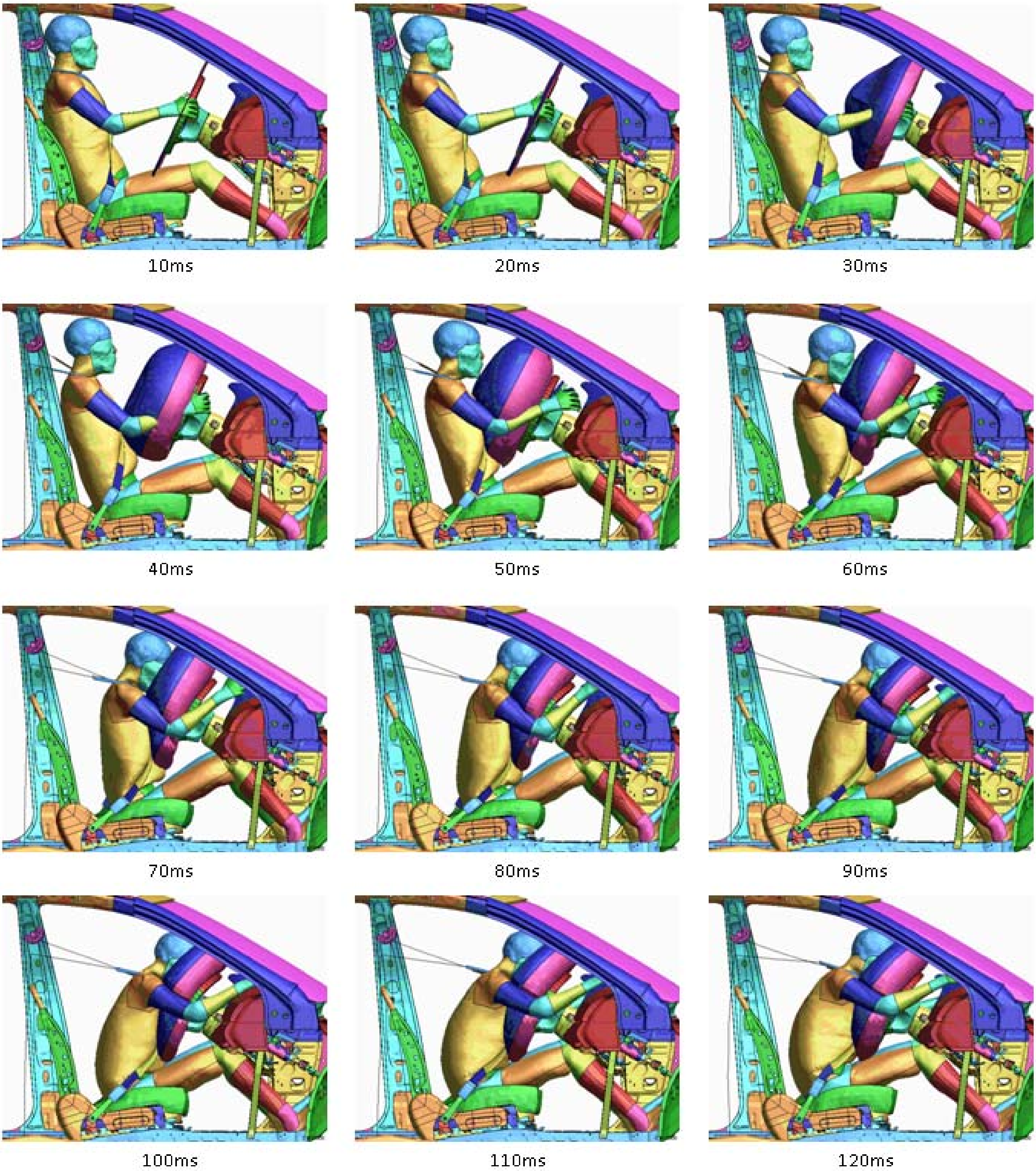

Fig. A5. Occupant Kinematics of AM50 Occupant with Four-Point Seatbelt (Case 20).

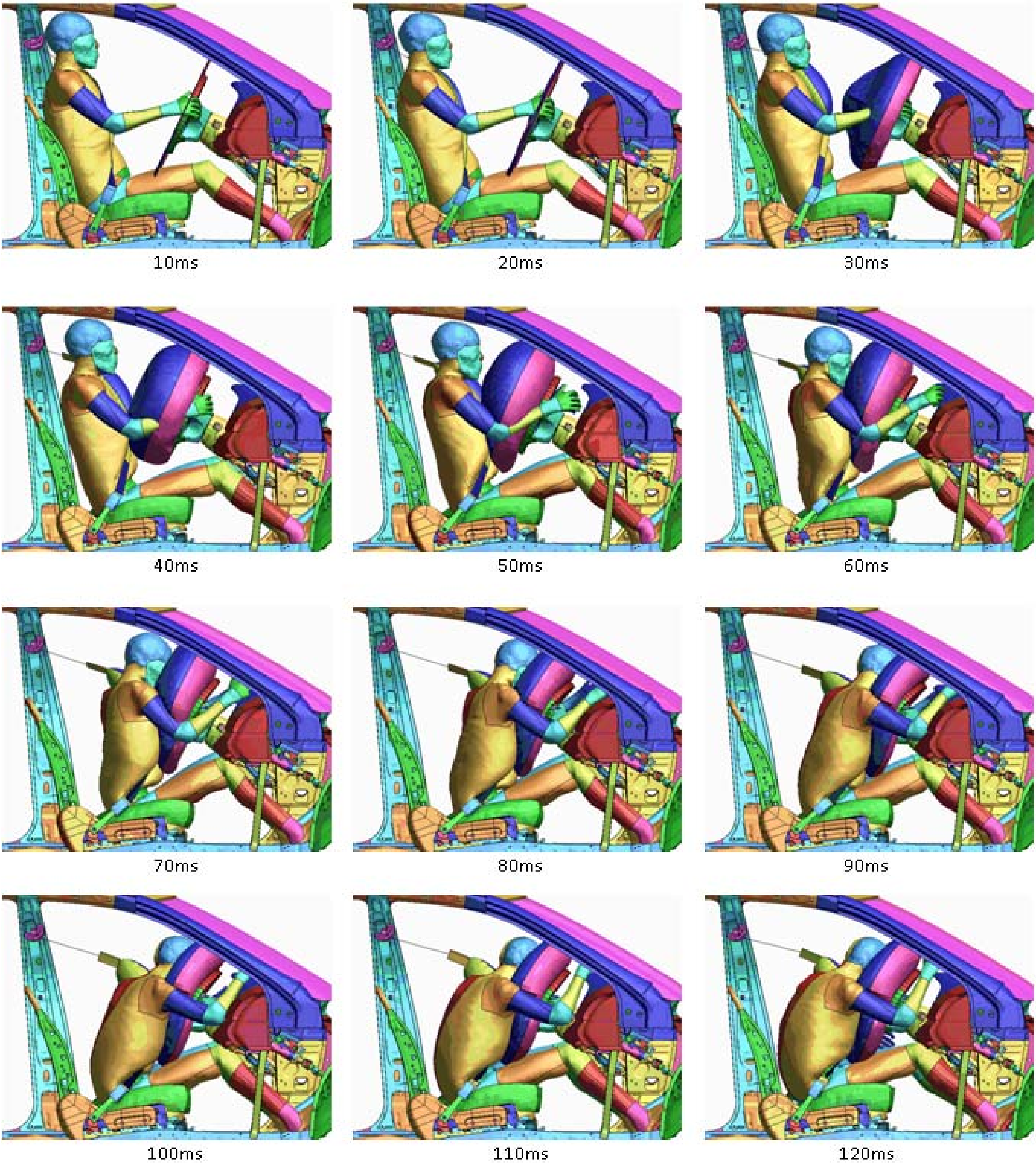

Fig. A6. Occupant Kinematics of AM50 Occupant with Airbelt (Case 21).

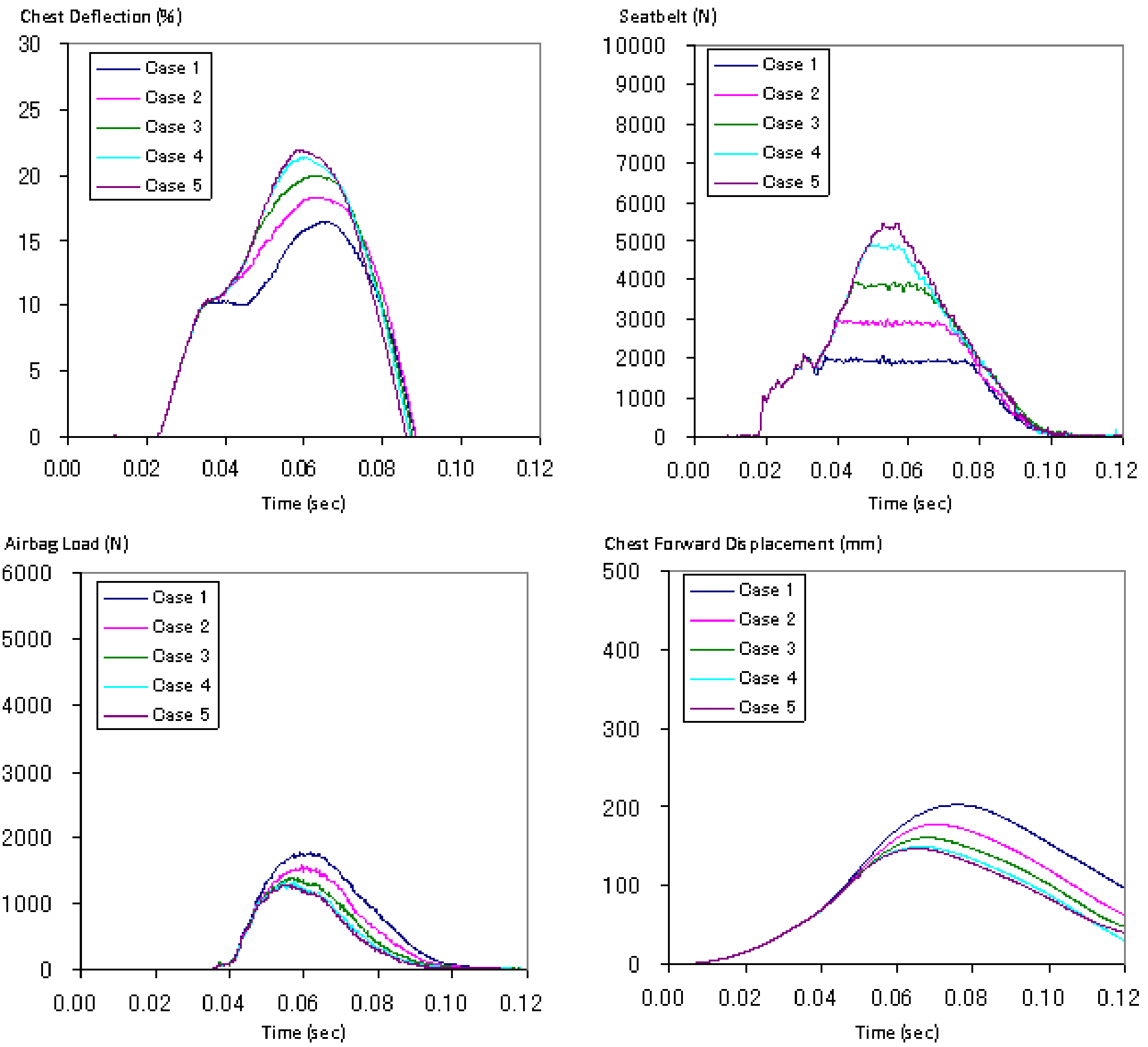

Fig. A7. Chest Deflection, Seatbelt Load, Airbag Load and Chest Forward Displacement of AF05 Occupant with Different Load Limiter Values (Case 1-5).

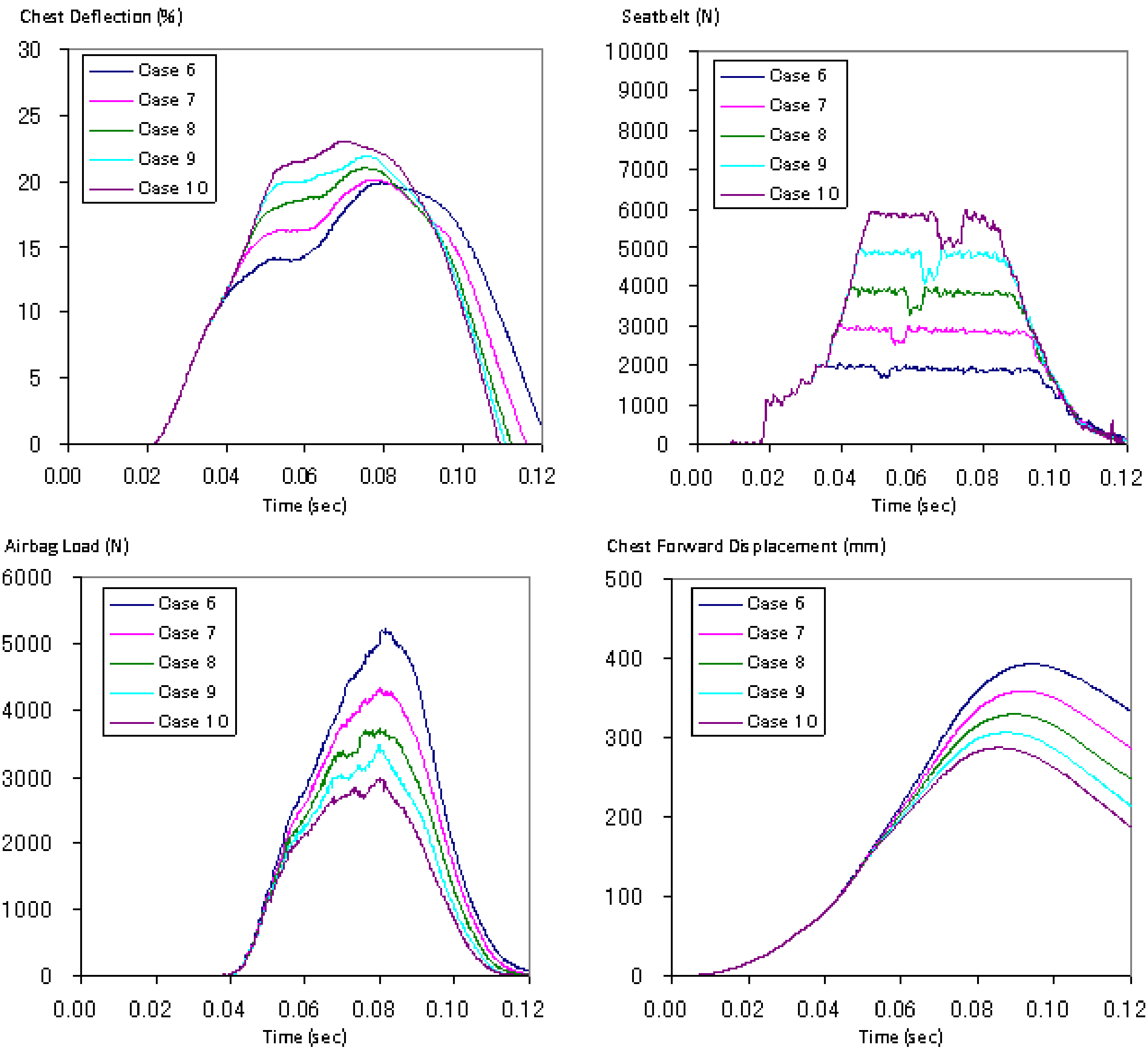

Fig. A8. Chest Deflection, Seatbelt Load, Airbag Load and Chest Forward Displacement of AM50 Occupant with Different Load Limiter Values (Case 6-10).

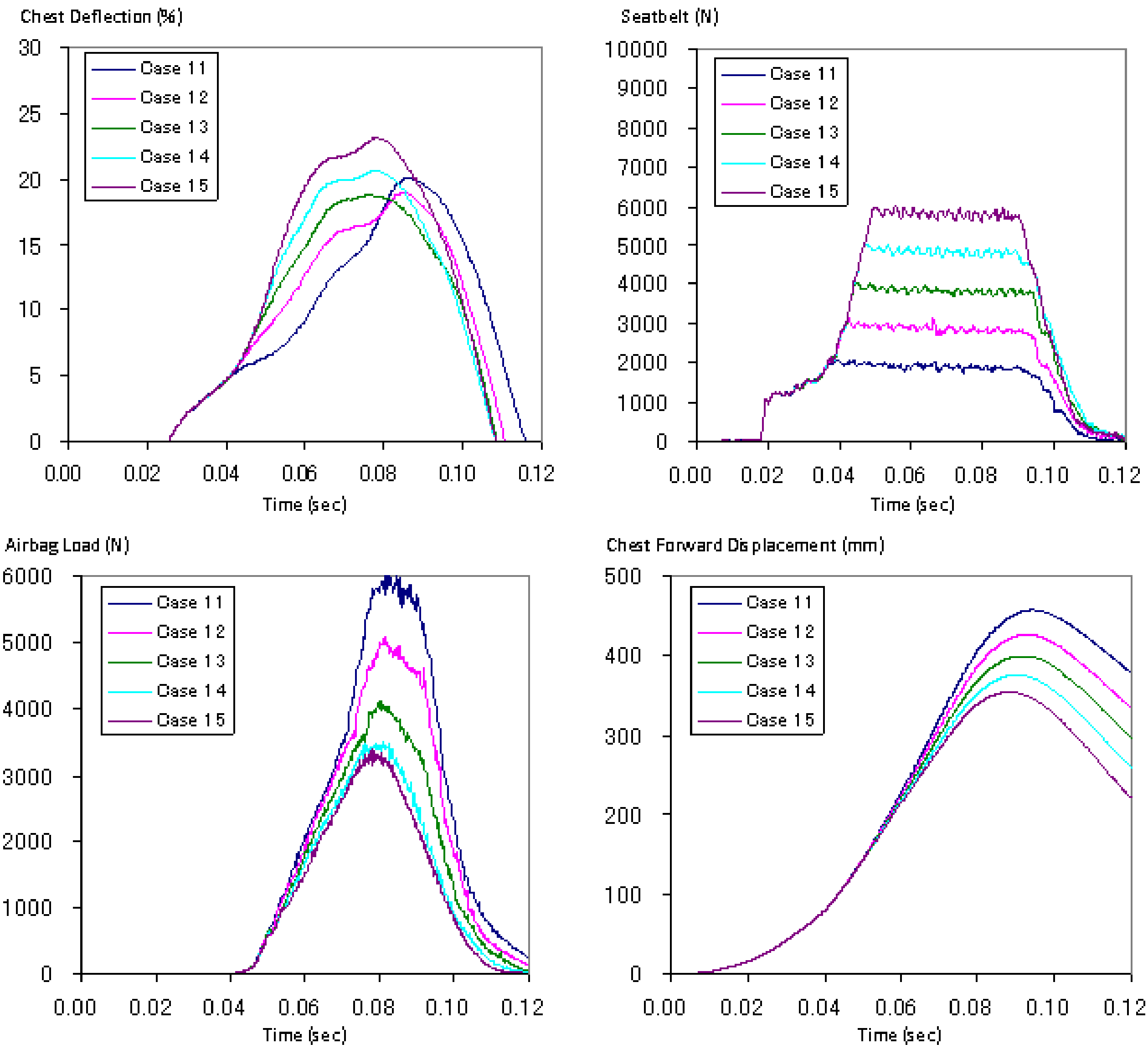

Fig. A9. Chest Deflection, Seatbelt Load, Airbag Load and Chest Forward Displacement of AM95 Occupant with Different Load Limiter Values (Case 11-15).

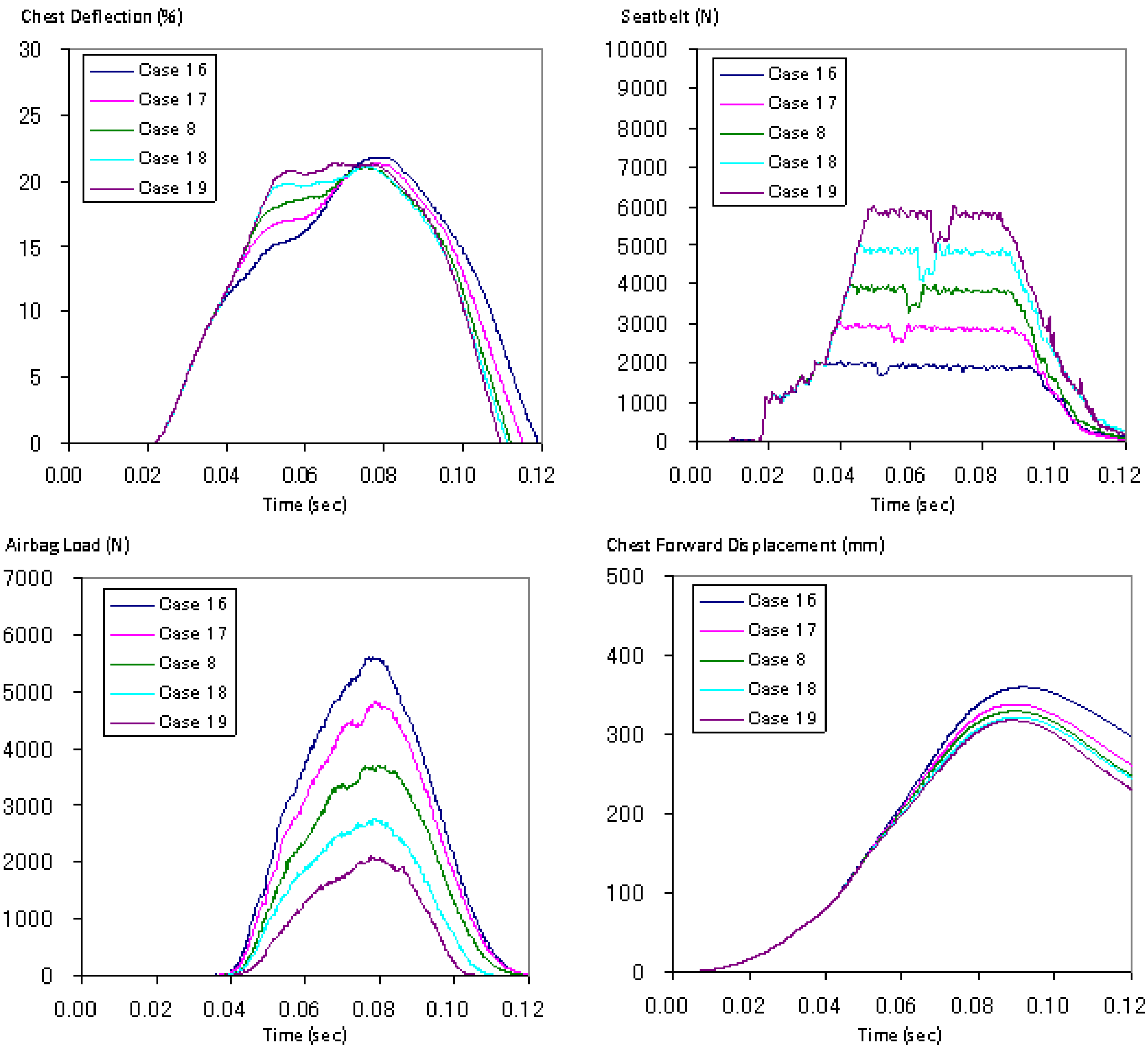

Fig. A10. Chest Deflection, Seatbelt Load, Airbag Load and Chest Forward Displacement of AM50 Occupant with Different Load Limiter Values (Case 16-19).

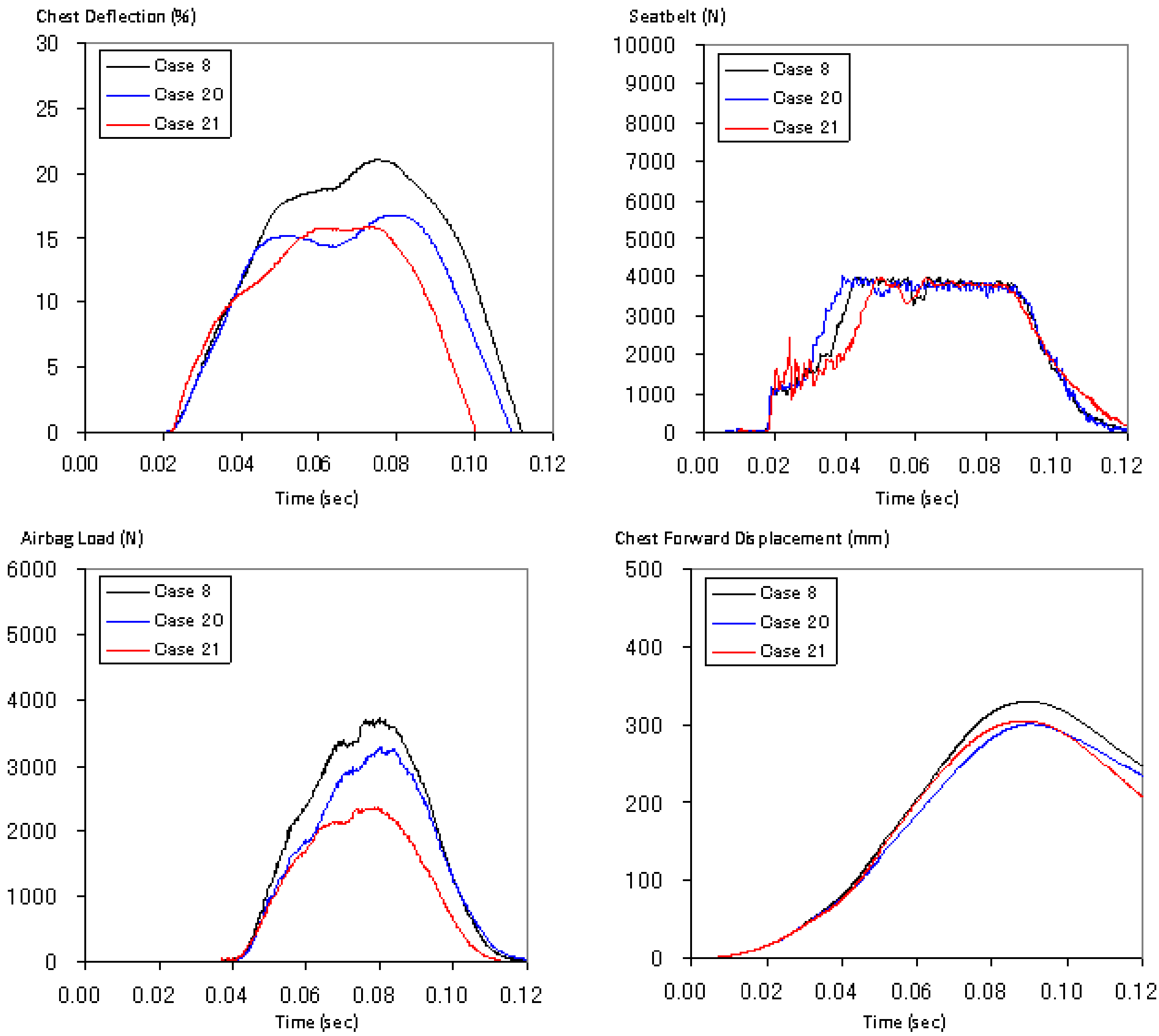

Fig. A11. Comparison of Chest Deflection, Seatbelt Load, Airbag Load and Chest Forward Displacement between Different Seatbelt Types (Case 8, 20 and 21).

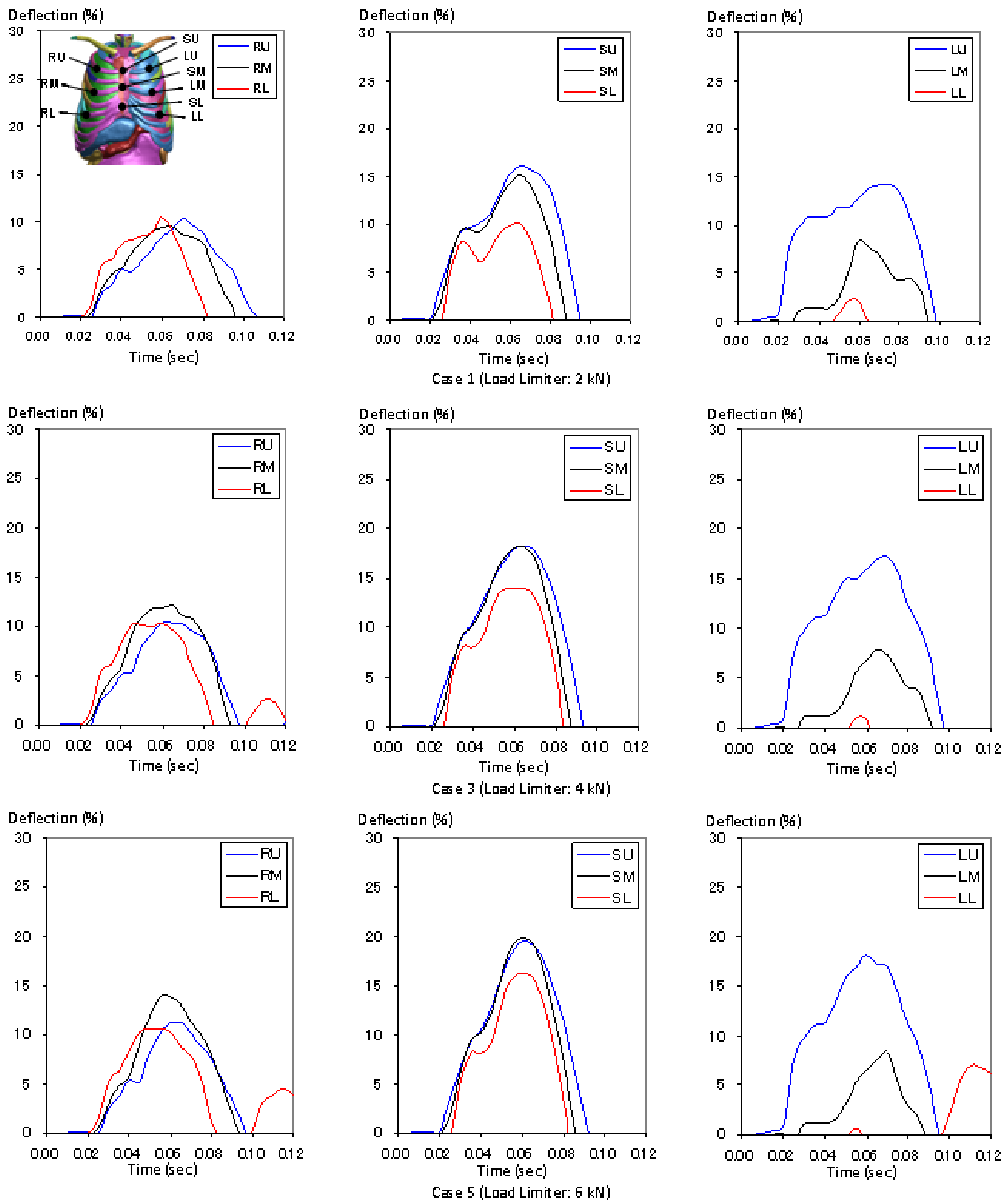

Fig. A12. Local Chest Deflection of AF05 Occupant with Different Load Limiter Values (Case 1, 3 and 5).

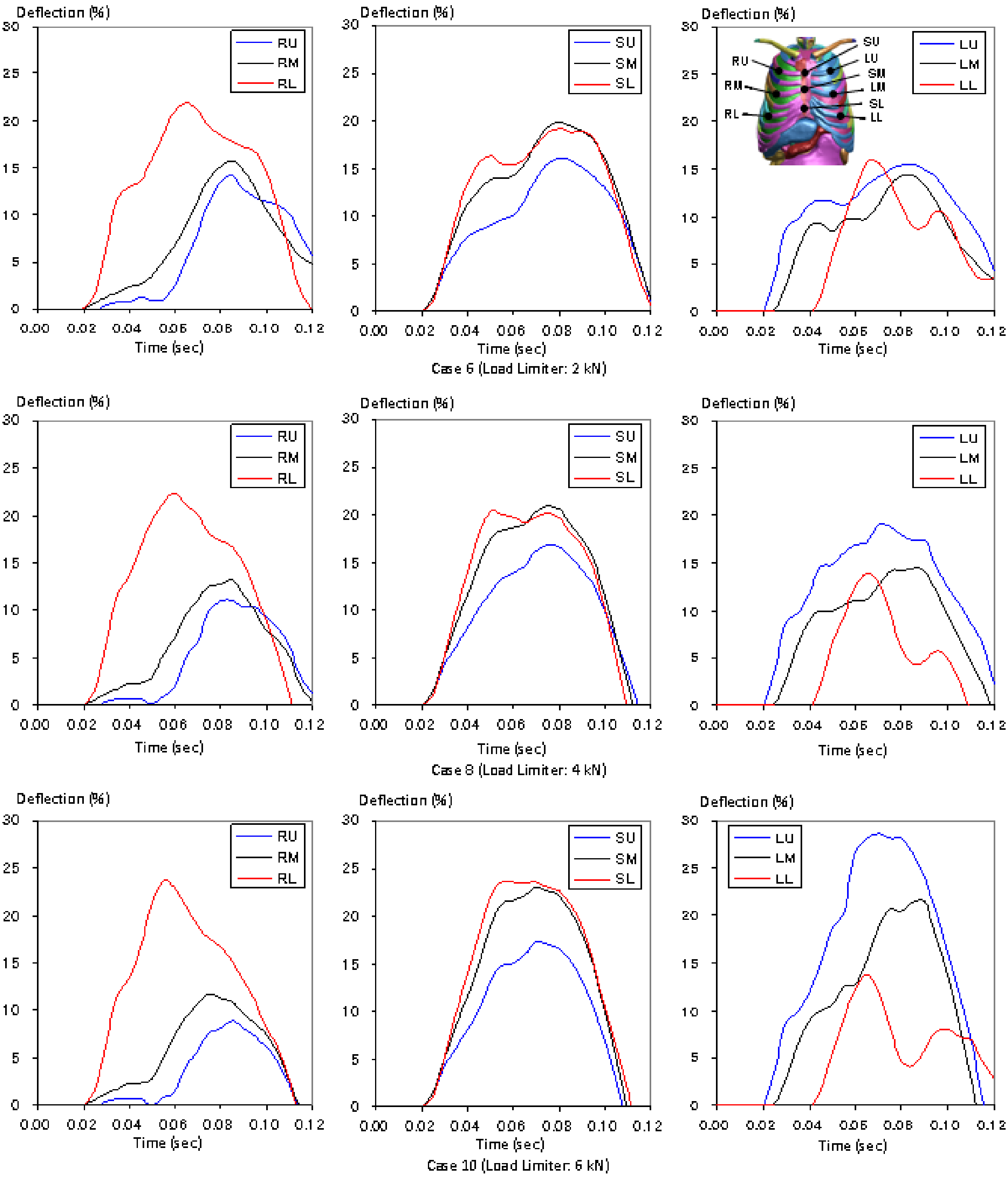

Fig. A13. Local Chest Deflection of AM50 Occupant with Different Load Limiter Values (Case 6, 8 and 10).

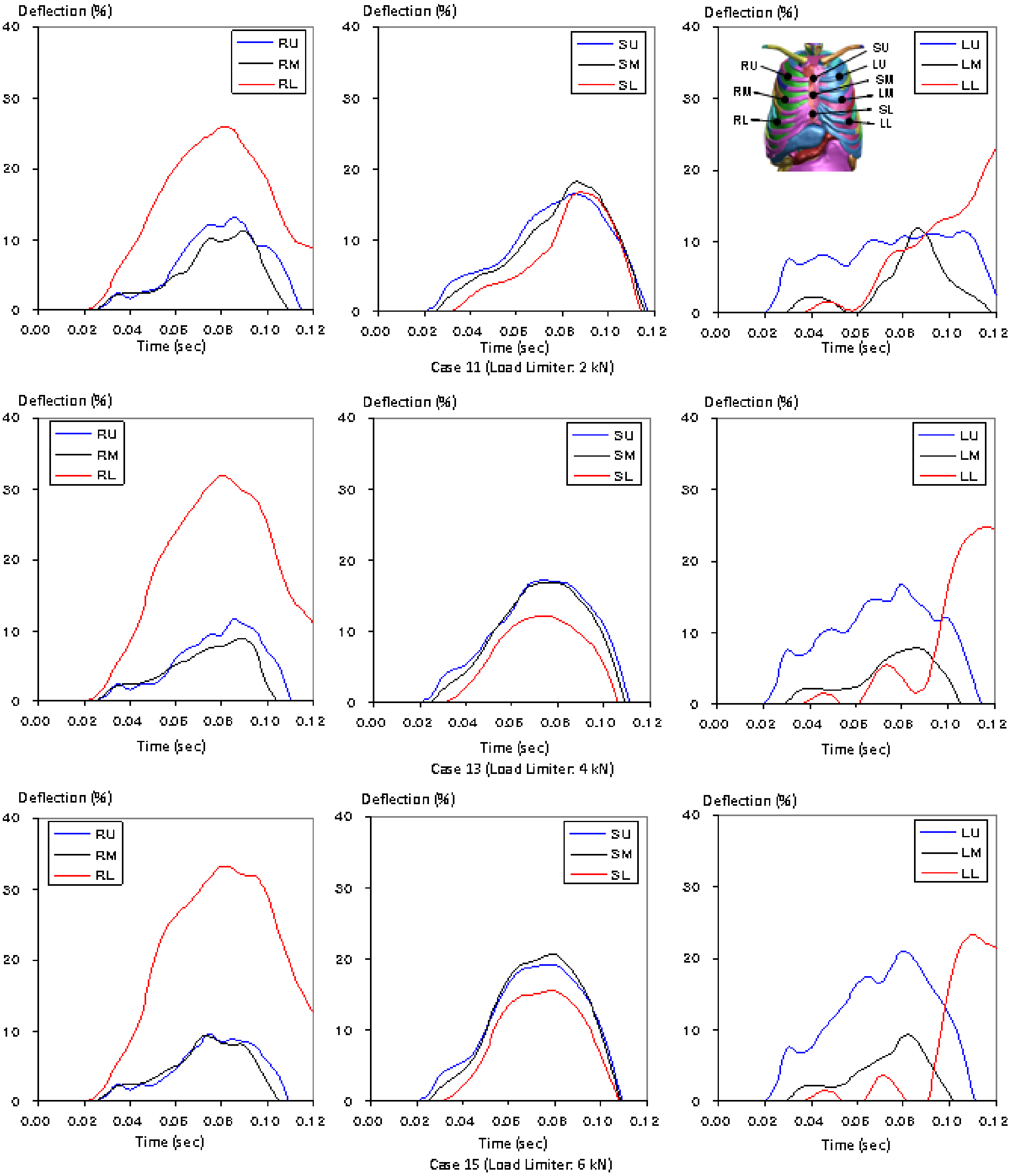

Fig. A14. Local Chest Deflection of AM95 Occupant with Different Load Limiter Values (Case 11, 13 and 15).

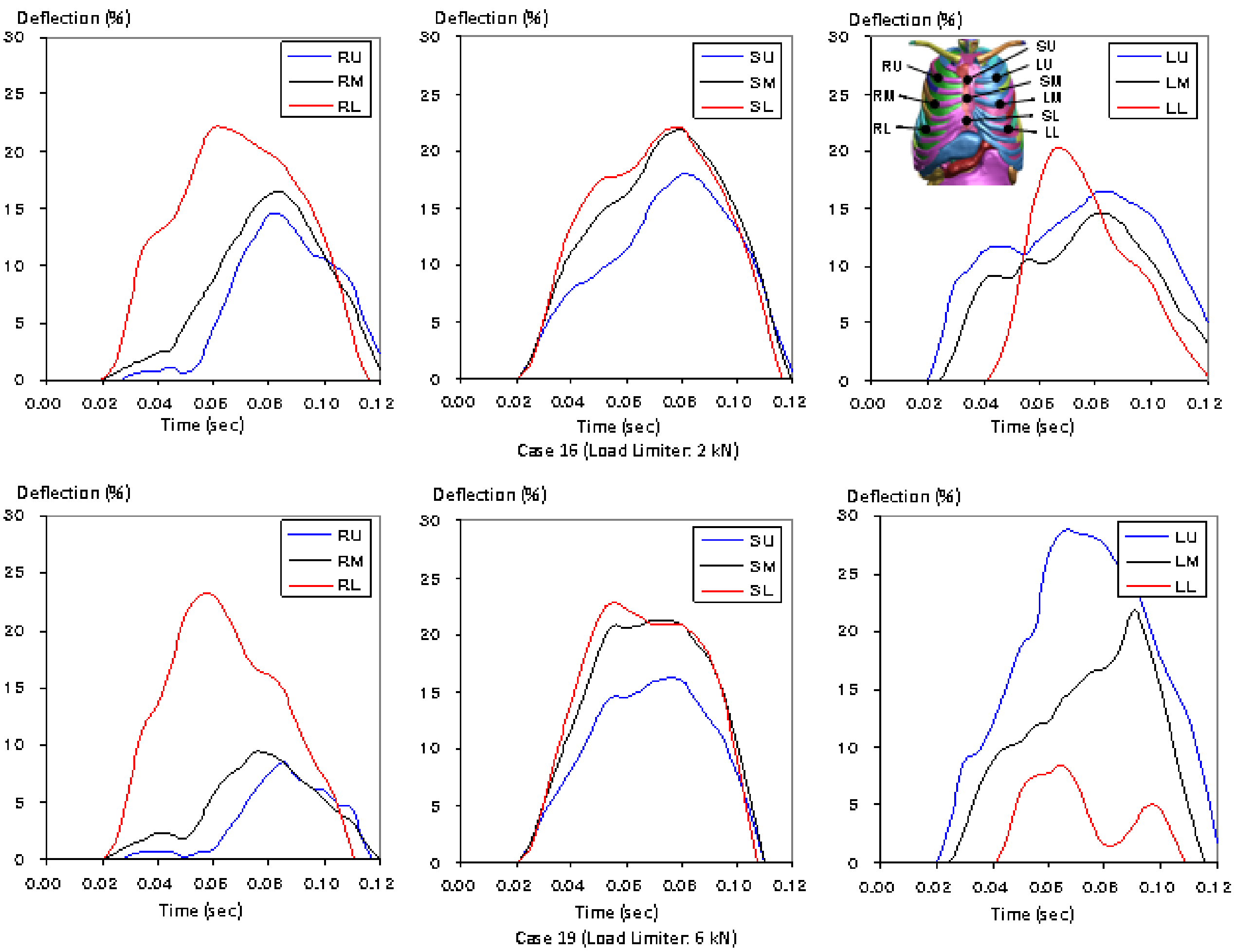

Fig. A15. Local Chest Deflection of AM50 Occupant with Different Load Limiter Values (Case 16 and 19).

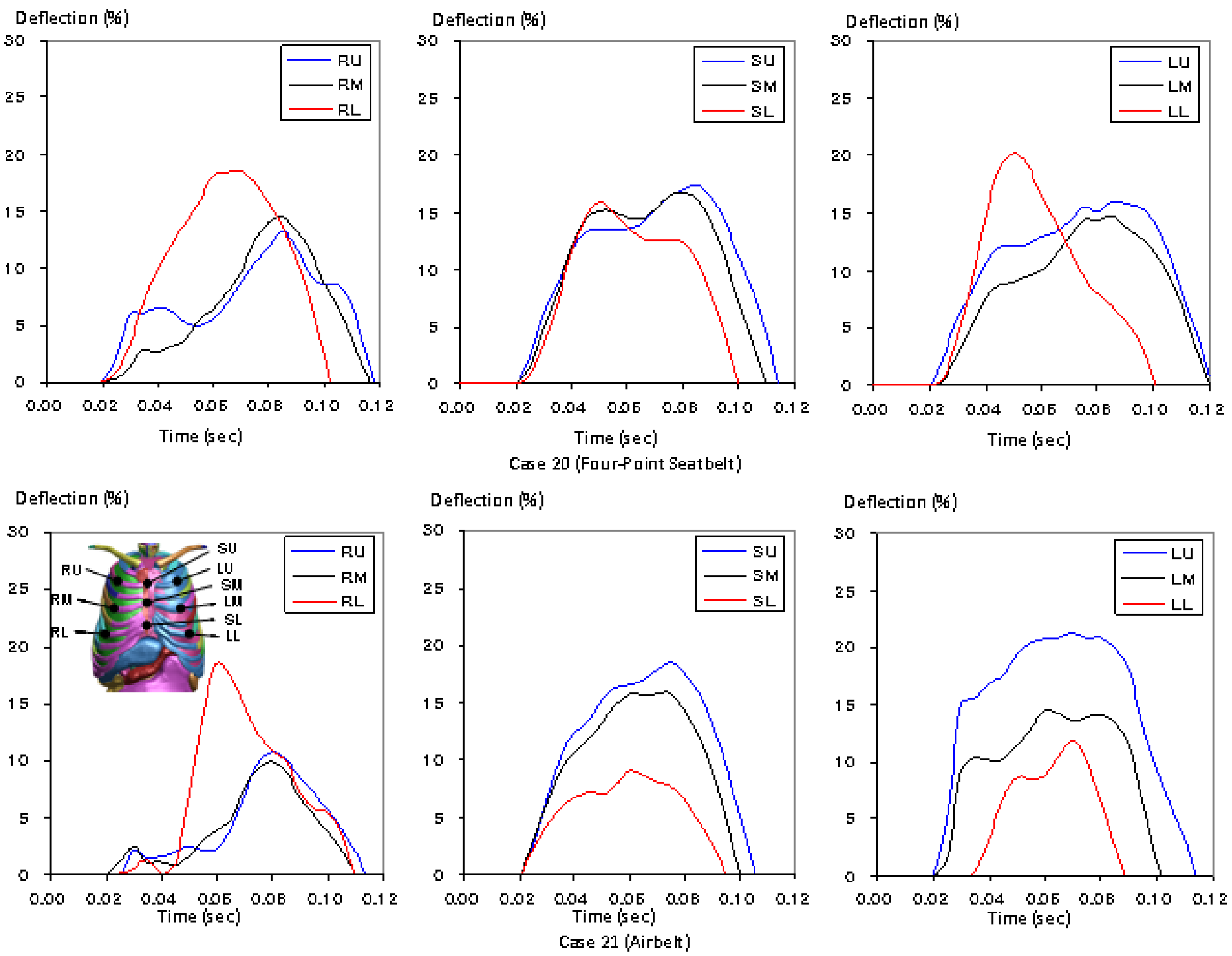

Fig. A16. Local Chest Deflection of AM50 Occupant with Different Seatbelt Types (Case 20 and 21).

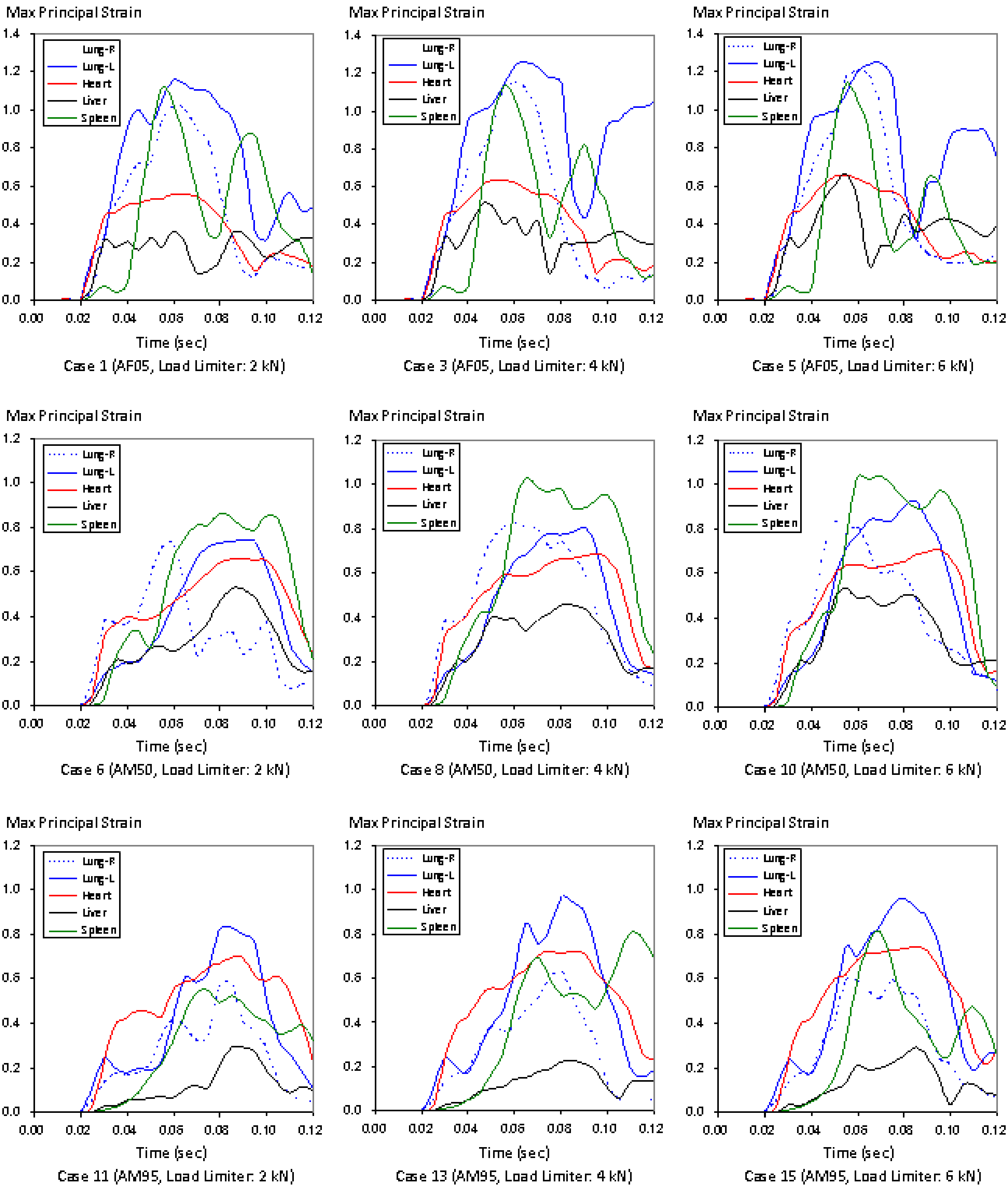

Fig. A17. Max Principal Strain of Internal Organs (Case 1,3, 5, 6, 8, 10, 11, 13 and 15).

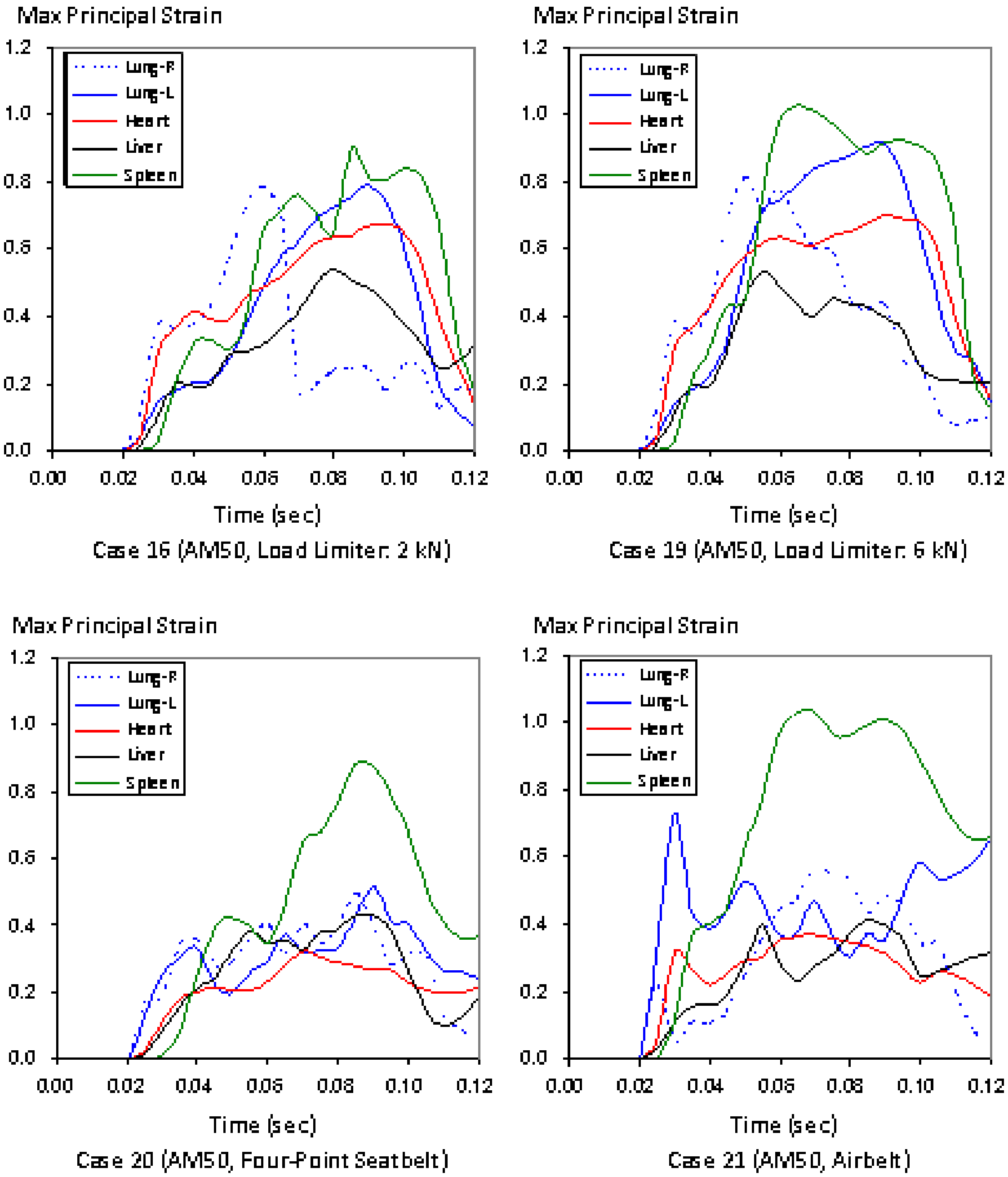

Fig. A18. Max Principal Strain of Internal Organs (Case 16, 9, 20 and 21).

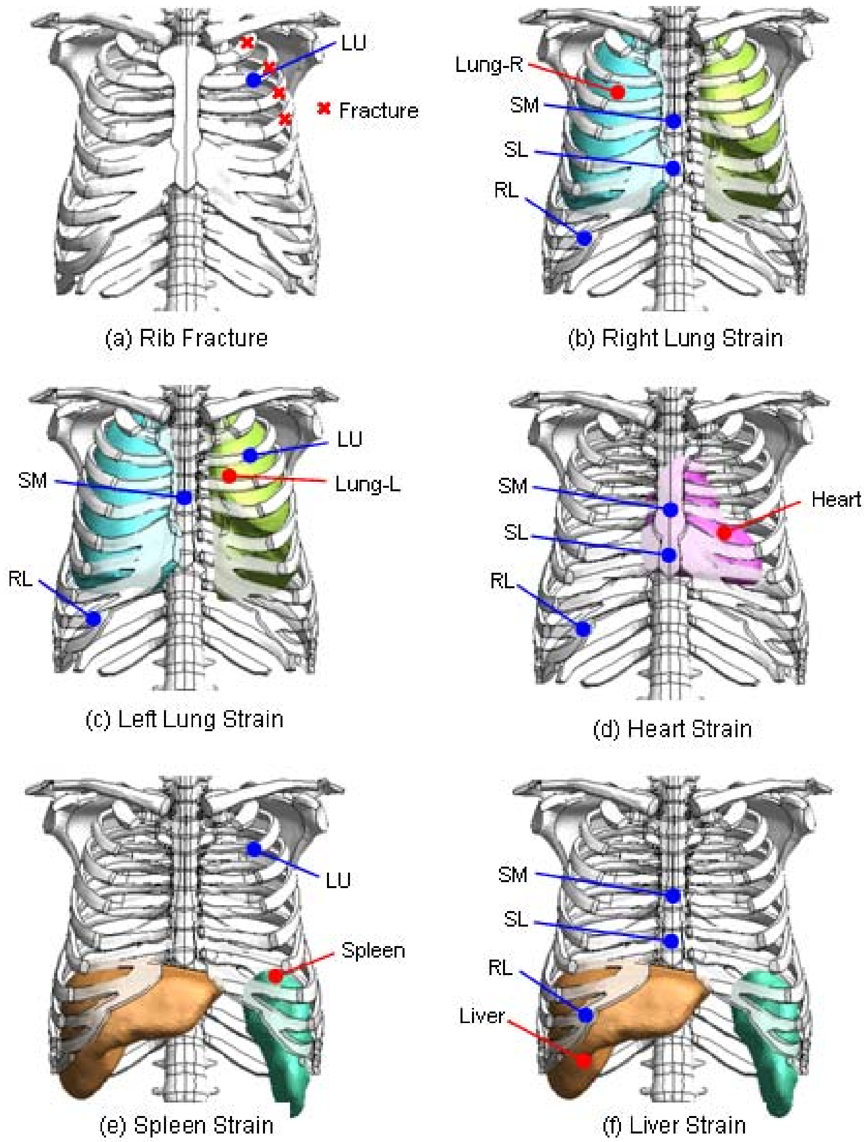

Fig. A19. Correlation between Local Chest Deflections and Injury Values.

TABLE AI

Max Values of Chest Deflection, Seatbelt Load, Airbag Load, Forward Displacement and No. of Rib Fractures

Case	Occupant	Load Limiter	Chest Def.	Seatbelt Load	Airbag Load	F. Displ	Rib FX
1	AF05	2kN	16.5%	1921N	1784N	201mm	-
2		3kN	18.2%	2892N	1591N	177mm	-
3		4kN	20.0%	3163N	1409N	160mm	-
4		5kN	21.3%	3193N	1329N	149mm	-
5		6kN	21.9%	3391N	1302N	147mm	-
6	AM50	2kN	19.9%	1914N	5236N	393mm	-
7		3kN	20.1%	2892N	4334N	359mm	-
8		4kN	21.1%	3776N	3721N	330mm	L1
9		5kN	21.9%	4788N	3485N	307mm	L1,L2,L3
10		6kN	23.0%	5201N	2969N	288mm	L1,L2,L3,L4
11	AM95	2kN	20.1%	1926N	5812N	457mm	-
12		3kN	19.0%	2745N	4947N	427mm	-
13		4kN	18.8%	3896N	4081N	400mm	-
14		5kN	20.7%	4880N	3493N	376mm	-
15		6kN	23.2%	5691N	3395N	355mm	-
16	AM50	2kN	19.9%	1936N	5614N	360mm	L1
17		3kN	20.1%	2836N	4831N	339mm	L1
18		5kN	21.9%	4871N	2746N	323mm	L1,L2,L3
19		6kN	23.0%	5100N	2088N	319mm	L1,L2,L3
20	4-Point	2kN+2kN	16.8%	4032N	3290N	301mm	-
21	Airbelt	4kN	15.9%	3973N	2361N	305mm	L1

TABLE AII
Max Values of Local Chest Deflections at Nine Calculation Points

Case	RU	RM	RL	SU	SM	SL	LU	LU	LU
1	10.3	9.5	10.4	16.0	15.0	10.1	14.2	8.3	2.2
2	9.9	10.5	10.3	17.1	16.6	12.2	16.1	8.9	1.7
3	10.4	12.1	10.3	18.3	18.1	14.0	17.2	7.9	1.0
4	11.0	13.5	11.2	19.2	19.5	15.6	17.1	7.6	4.9
5	11.3	14.0	10.7	19.5	19.9	16.3	18.1	8.3	7.0
6	14.1	15.6	21.8	16.0	19.9	19.1	15.5	14.4	15.7
7	12.7	14.3	21.9	16.2	20.0	19.3	16.7	14.0	15.0
8	11.1	13.3	22.5	16.9	21.0	20.4	19.0	14.4	13.9
9	9.9	11.7	22.5	17.2	21.9	22.0	25.7	17.1	13.8
10	9.0	11.7	23.6	17.2	23.0	23.5	28.6	21.4	13.8
11	13.1	11.2	25.9	16.6	18.1	16.5	11.4	11.7	23.0
12	12.8	9.8	30.1	17.0	17.2	13.3	13.6	10.7	23.0
13	11.6	8.8	32.0	17.1	16.9	12.3	16.6	7.8	24.7
14	9.8	8.6	32.9	18.4	18.5	13.7	17.8	7.4	25.6
15	9.5	9.1	33.3	19.3	20.7	15.5	21.1	9.1	23.2
16	14.4	16.4	22.1	17.9	21.7	21.9	16.4	14.5	20.1
17	13.2	15.0	22.3	17.2	21.2	20.9	16.9	14.3	17.4
18	9.4	10.5	22.3	16.7	21.1	21.7	25.8	16.4	12.0
19	8.6	9.4	23.1	16.2	21.2	22.7	28.7	21.9	8.5
20	13.4	14.5	18.6	17.4	16.7	15.9	15.9	14.8	20.2
21	10.7	10.0	18.4	18.4	15.8	9.0	21.3	14.5	11.8

TABLE AIII
Max Principal Strain Values of Internal Organs

Case	Lung-R	Ling-L	Heart	Spleen	Liver
1	1.02	1.15	0.56	1.12	0.36
2	1.05	1.24	0.62	1.15	0.45
3	1.15	1.26	0.64	1.13	0.51
4	1.19	1.28	0.65	1.11	0.61
5	1.20	1.24	0.66	1.14	0.67
6	0.72	0.74	0.66	0.86	0.53
7	0.82	0.78	0.68	0.95	0.46
8	0.82	0.81	0.69	1.03	0.46
9	0.80	0.89	0.71	1.04	0.49
10	0.83	0.93	0.71	1.04	0.54
11	0.57	0.83	0.70	0.55	0.29
12	0.62	0.87	0.70	0.64	0.27
13	0.63	0.97	0.72	0.81	0.23
14	0.67	1.00	0.75	0.72	0.24
15	0.59	0.96	0.74	0.81	0.29
16	0.78	0.79	0.68	0.90	0.54
17	0.81	0.79	0.69	0.91	0.48
18	0.81	0.90	0.70	1.07	0.47
19	0.81	0.92	0.70	1.03	0.53
20	0.49	0.52	0.32	0.88	0.43
21	0.57	0.73	0.37	1.03	0.42